

Ridge Regression with Frequent Directions: Statistical and Optimization Perspectives

Charlie Dickens
University of Warwick

Abstract

Despite its impressive theory & practical performance, Frequent Directions (FD) has not been widely adopted for large-scale regression tasks. Prior work has shown randomized sketches (i) perform worse in estimating the covariance matrix of the data than FD; (ii) incur high error when estimating the bias and/or variance on sketched ridge regression. We give the first constant factor relative error bounds on the bias & variance for sketched ridge regression using FD. We complement these statistical results by showing that FD can be used in the optimization setting through an iterative scheme which yields high-accuracy solutions. This improves on randomized approaches which need to compromise the need for a new sketch every iteration with speed of convergence. In both settings, we also show using *Robust Frequent Directions* further enhances performance.

1 Introduction

Ridge regression (RR) has become a key tool in data analysis but it is resource intensive to solve at large scale and in high dimensions. Recall that the RR problem is to return:

$$\min_{\mathbf{x} \in \mathbb{R}^d} \left\{ f(\mathbf{x}) = \frac{1}{2} \|\mathbf{A}\mathbf{x} - \mathbf{b}\|_2^2 + \frac{\gamma}{2} \|\mathbf{x}\|_2^2 \right\} \quad (1)$$

Solving (1) when $n > d$ by the SVD (or other related decompositions) requires $O(nd^2)$ time and $O(d^2)$ space. These complexities are not acceptable given the scale of modern data.

A crucial quantity in both solving and approximat-

ing RR is the *Hessian*¹ matrix $\mathbf{H}_\gamma = \mathbf{A}^\top \mathbf{A} + \gamma \mathbf{I}_d$. Maintaining \mathbf{H}_γ exactly by rank-one updates of the samples costs $O(nd^{\omega-1})$ time and $O(d^2)$ space so offers little overall benefit. Speeding up this computation has been studied through *randomized* matrix sketching techniques which estimate \mathbf{H}_γ through $\tilde{\mathbf{H}}_\gamma = \mathbf{A}^\top \mathbf{S}^\top \mathbf{S} \mathbf{A} + \gamma \mathbf{I}_d$. Provided that $\mathbf{S} \in \mathbb{R}^{m \times n}$ is sampled from a suitable distribution (details in (Woodruff, 2014; Drineas & Mahoney, 2016)), then $\tilde{\mathbf{H}}_\gamma$ is a good proxy for \mathbf{H}_γ . The computational savings come when \mathbf{S} can be applied to input \mathbf{A} quickly or implicitly as the data is read.

The exact solution to (1) is given in (2). There are two central “one-shot” methods to approximate (1): *Classical* (3) (Avron et al., 2017) and *Hessian* (4) (Pilanci & Wainwright, 2015) Sketching:

$$\mathbf{x}^* = (\mathbf{A}^\top \mathbf{A} + \gamma \mathbf{I}_d)^{-1} \mathbf{A}^\top \mathbf{y} \quad (2)$$

$$\mathbf{x}^C = (\mathbf{A}^\top \mathbf{S}^\top \mathbf{S} \mathbf{A} + \gamma \mathbf{I}_d)^{-1} \mathbf{A}^\top \mathbf{S}^\top \mathbf{S} \mathbf{y} \quad (3)$$

$$\mathbf{x}^H = (\mathbf{A}^\top \mathbf{S}^\top \mathbf{S} \mathbf{A} + \gamma \mathbf{I}_d)^{-1} \mathbf{A}^\top \mathbf{y} \quad (4)$$

If sketching the data to obtain $\mathbf{S}\mathbf{A}$ takes time T_{sketch} , then approximating (1) is $O(T_{\text{sketch}} + md^2)$ time. As² $m = \tilde{O}(d \text{ poly } \log(d))$ the space grows as $\tilde{O}(d^2)$.

When ridge regression is practical, one often finds redundancy in the spectrum of high-dimensional input data. Hence, it would be ideal to perform an online or streaming variant of SVD keeping only the informative parts of the spectrum. Unfortunately, greedy heuristics (Brand, 2002) can be shown to perform arbitrarily badly (Huang, 2018). Liberty (2013) introduced Frequent Directions (FD) for exactly this problem; to find a matrix summary $\mathbf{B} \in \mathbb{R}^{m \times d}$ that well approximates the information one would obtain from performing an SVD of \mathbf{A} . Therefore, FD is a natural candidate sketch for approximating ridge regression.

Frequent Directions is an orthogonal approach to ran-

¹Due to the fact it is the matrix of second derivatives of $f(\mathbf{x})$ in (1). It is composed of the data covariance $\mathbf{A}^\top \mathbf{A}$ and a regularization term $\gamma \mathbf{I}_d$.

²The \tilde{O} notation suppresses lower order and failure probability terms

* Work done while at DataSketches, Verizon Media.

domized matrix sketching. FD *deterministically* updates the top singular directions observed in the data stream, keeping only the most important (or the most frequently occurring). In Ghashami et al. (2016b), compelling evidence was given that showed FD more accurately approximates $\mathbf{A}^\top \mathbf{A}$ at a given projection dimension m than randomized methods. FD is also a mergeable summary (Agarwal et al., 2013), and can be adapted to sparse data (Ghashami et al., 2016a). Given that $\mathbf{H}_\gamma = \mathbf{A}^\top \mathbf{A} + \gamma \mathbf{I}_d$ is a fundamental operator in RR, one would hope that FD can be used as the sketch here, rather than random projection. Indeed, this is shown in Shi & Phillips (2020) who use $\hat{\mathbf{H}} = \mathbf{B}^\top \mathbf{B} + \gamma \mathbf{I}_d$ to approximate \mathbf{H}_γ . If the interplay between the regularisation γ and the approximation error from FD are correctly balanced, then \mathbf{x}^* can be reasonably approximated. We refer to this approach as *Frequent Directions Ridge Regression (FDRR)* (Alg. A2, App. A) returning $\hat{\mathbf{x}} = \hat{\mathbf{H}}^{-1} \mathbf{A}^\top \mathbf{y}$.

However, it remains the case that despite being a high-quality sketch, FD is under-exploited in regression tasks. Our motivation is to better understand how FD can be used in regression and what properties it preserves. We are interested in the following questions which prior work has failed to address:

1. **Statistical model estimation.** Ridge regression is often studied under a linear model with a ground truth vector \mathbf{x}_0 that describes the behavior of the data. If FD is employed as the sketch, then how does this distort the bias and variance of the returned weights compared to the “optimal” bias and variance in recovering \mathbf{x}_0 ?
2. **Solution estimation.** Can the coarse approximation of \mathbf{x}^* from Shi & Phillips (2020) be bootstrapped to obtain a high accuracy estimate $\hat{\mathbf{x}}$?

These two questions underpin complementary perspectives commonly found in the machine learning community. The former is a *statistical perspective* while the latter is an *optimization perspective*. It is argued in Wang et al. (2017) that *both* are of importance in theory and practice depending on the application. The statistical perspective is relevant in machine learning when the approximate solution $\hat{\mathbf{x}}$ is used as a proxy for the optimal weights \mathbf{x}^* which are too expensive to obtain. Meanwhile, the optimization perspective is useful when one wishes to understand how sequentially refining expensive iterations can lead to better estimates of the solution vector.

1.1 Contributions

Our contributions are two-fold:

1. **Statistical results:** we give the first analysis for FDRR under a linear model. We provide constant factor relative error bounds on the bias, variance,

and mean-squared error (MSE). For a $\theta \in (0, 1)$, we find that $(1 - \theta) \|\text{bias}(\mathbf{x}^*)\|_2^2 \leq \|\text{bias}(\hat{\mathbf{x}})\|_2^2 \leq \|\text{bias}(\mathbf{x}^*)\|_2^2 / (1 - \theta)$, likewise for trace of variance and MSE. We show that using the more accurate *Robust Frequent Directions* (Huang, 2018) improves this to a $1 - \theta'$ approximation for $\theta' < \theta$.

2. **Optimization results:** we present the first analysis of FD in an iterative scheme to obtain *high-quality solution estimation*. We show that t iterates $\mathbf{x}^{(t)} = \mathbf{x}^{(t-1)} - \hat{\mathbf{H}}^{-1} \nabla f(\mathbf{x}^{(t)})$ yields weights $\hat{\mathbf{x}} = \mathbf{x}^{(t)}$ satisfying $\|\hat{\mathbf{x}} - \mathbf{x}^*\|_2 \leq \zeta^t \|\mathbf{x}^*\|_2$. This can substantially improve the one-shot sketch estimate $\hat{\mathbf{x}} = \mathbf{x}^{(1)}$ of Shi & Phillips (2020) even if t is small or moderate.

Although these results are simple, there are significant practical implications. From the statistical side, our results show that FDRR returns weights which are much more faithful to the underlying model than randomized sketching: this is highlighted in Table 1. If the bias-variance tradeoff is a key concern then FDRR should be preferred to using random projections. Secondly, on the optimization side, we show the existence of small-space deterministic preconditioners which can be iteratively used to refine the estimates to ridge regression. The significance of our results is that FDRR requires space only $O(md)$ for $m < d$ by storing $\mathbf{B} \in \mathbb{R}^{m \times d}$ and some extra information such as $\mathbf{A}^\top \mathbf{y}$. Consequently, FDRR can operate in higher dimensions than randomized methods which need $\mathbf{SA} \in \mathbb{R}^{\tilde{O}(d) \times d}$.

1.2 Related Work

Although we are not the first to study FD in regression tasks, prior work has different motivations, presents *complementary* results to ours, and thus uses different techniques. Shi & Phillips (2020) introduced FDRR, returning $\hat{\mathbf{x}}$ which satisfies a coarse bound $\|\hat{\mathbf{x}} - \mathbf{x}^*\| \leq \zeta \|\mathbf{x}^*\|$ in $O(d/\zeta)$ space. Let $m = O(1/\zeta) < d$ be the number of rows in (and the rank of) \mathbf{B} . Since $\hat{\mathbf{H}} = \mathbf{B}^\top \mathbf{B} + \gamma \mathbf{I}_d$, Shi & Phillips (2020) show that using an eigendecomposition of $\hat{\mathbf{H}}$ can be used to obtain $\hat{\mathbf{H}}^{-1}$ in $O(md)$ which results in the first $o(d^2)$ streaming algorithm to estimate \mathbf{x}^* .

However, this results fails to provide any information on the model estimation provided by $\hat{\mathbf{x}}$ performs under the linear model we study. Until this work nothing was known about the statistical performance of sketched ridge regression using FD. We seek strong statistical guarantees on the bias and variance of $\hat{\mathbf{x}}$ when compared to the same quantities had no sketching been performed. Alternatively, Huang (2018) propose using FD for *adversarial online learning* through an approximate Newton method. Hence, their application and bounds are much different from ours; no bounds on the solution estimation $\|\hat{\mathbf{x}} - \mathbf{x}^*\|_2$ are provided.

Method	$\ \text{bias}(\hat{\mathbf{x}})\ _2^2$		$\text{trace}(\text{var}(\mathbf{x}))$		Time	Space (num. rows m)
	LB	UB	LB	UB		
FDRR	$1 - \theta$	$1/1-\theta$	$1 - \theta$	$1/1-\theta$	$O(ndm)$	$O(md)$
RFDRR	$1 - \theta'$	$1/1-\theta'$	$1 - \theta'$	$1/1-\theta'$	$O(ndm)$	$O(md)$
Classical	$1/(1+\rho)^2$	$1/(1-\rho)^2$	$c_1 \frac{n(1-\rho)}{m(1+\rho)^2}$	$c_2 \frac{n(1+\rho)}{m(1-\rho)^2}$	$O(\text{nnz}(\mathbf{A})) \sim O(nd^2)$	$\tilde{O}(d\rho^{-2} \text{poly log } d)$
Hessian	$c'_1 \frac{\rho}{1+\rho}$	$c'_2 \rho(1+\rho)$	$1/(1+\rho)^2$	$1/(1-\rho)^2$	$O(\text{nnz}(\mathbf{A})) \sim O(nd^2)$	$\tilde{O}(d\rho^{-2} \text{poly log } d)$

Table 1: Lower (LB) & upper (UB) bounds for bias & variance of competing sketching methods. Deterministic methods require $m = \|\mathbf{A} - \mathbf{A}_k\|_F^2 / (1 - \sqrt{1 - \theta})^\gamma + k < d$ rows. Bounds for Classical/Hessian sketch are slight modifications of (Wang et al., 2017) for $(1 \pm \rho)$ - ℓ_2 subspace embeddings \mathbf{S} . Extra parameters are constants $c_1, c_2 \approx 1$ and singular values σ_j^2 of the input data. The constants c'_1, c'_2 are slightly more involved, (Wang et al., 2017) should be consulted for the details.

Randomized approaches for sketched ridge regression from the statistical setting typically exploit ℓ_2 -subspace embeddings which asserts that \mathbf{SA} has all directions of \mathbf{A} preserved up to some small relative error. However, this requires sampling $m = \tilde{O}(d \text{poly log } d)$ projections: a stronger condition than retaining only $m < d$ directions as in FD. A severe weakness of one-shot randomized sketching in the statistical setting is that only one of bias or variance can be well approximated: Classical sketch estimates well the bias but has significantly higher variance than the optimal solution while Hessian sketch has the opposite behaviour (Wang et al., 2017). It is also shown in Wang et al. (2017) that averaging the solutions to many sketched ridge regression problems can improve the bias and variance estimation. However, we are primarily interested in the ‘standard’ usage of one-shot sketching such as Classical and Hessian sketch which use only one sketch of the data. Thus, a comparison to the so-called *model-averaging* approach falls outside the scope of our study.

The central benefit of using FD for ridge regression is that $o(d^2)$ space is required to obtain approximation guarantees Shi & Phillips (2020). At a high level, this is due to the fact FD incurs less distortion in approximating $\mathbf{A}^\top \mathbf{A}$ by $\mathbf{B}^\top \mathbf{B}$ compared to a random projection $\mathbf{A}^\top \mathbf{S}^\top \mathbf{SA}$ when \mathbf{B} and \mathbf{SA} are of the same size. Random projections can still preserve much information when $m < d$ for problems such as approximate matrix product (Cohen et al., 2016); convex constrained least squares (Pilanci & Wainwright, 2015, 2016); underconstrained ridge regression (Chowdhury et al., 2018). However, we are not aware of any *statistical guarantees* on the bias-variance tradeoff of ridge regression when $m < d$ dimensions are kept in the sketch. Results in the optimization setting can be hindered by the need for a new sketch (even if it is of small-size) at every iteration Pilanci & Wainwright (2016). Using a single random sketch requires optimizing for the correct step size and

is only known to work for Gaussian random projections (Lacotte & Pilanci, 2019) which needs $O(nd^2)$ time to obtain \mathbf{SA} so is not a viable scalable solution.

Our Approach. Gaps in the existing literature mark our central departure from current work. Recall that in the statistical setting the task is to understand the model estimation (i.e., the mean-square error of $\hat{\mathbf{x}}$, to be defined formally in Section 2) meanwhile in the optimization setting we wish to minimise the solution estimation error $\|\hat{\mathbf{x}} - \mathbf{x}^*\|$.

In both statistical and optimization settings, randomized sketches have proven the most frequently studied technique. This is in spite of the superior practical performance FD provides in estimating $\mathbf{A}^\top \mathbf{A}$ shown in Ghashami et al. (2016b). Where FD has been studied, there has been no attempt to understand the statistical properties (bias, variance, MSE) which is crucial when using approximate weights $\hat{\mathbf{x}}$ in place of \mathbf{x}^* . Secondly, there has been no attempt to understand the performance of FD as a small-space preconditioners for high-accuracy solvers.

Paper Outline. Section 2 outlines the notation and sketching results we build upon. In Section 3 we present the statistical properties of (R)FDRR. Section 4 illustrates the iterative ridge sketching method. Both sections contain experiments to highlight the performance of our methods. The technical details & proofs are deferred to the appendix.

2 Preliminaries and Notation

Matrices of size $n \times d$ are denoted by uppercase letters e.g. $\mathbf{A} \in \mathbb{R}^{n \times d}$. The p -dimensional identity matrix is denoted by \mathbf{I}_p . Lower case symbols represent vectors, e.g. $\mathbf{x} \in \mathbb{R}^d$. The norms we use are the Frobenius norm $\|\mathbf{A}\|_F$, the spectral or operator norm over matrices $\|\mathbf{A}\|_2$ and Euclidean norm over vectors, $\|\mathbf{x}\|_2$.

Frequent Directions: Theoretical Properties
The property we exploit is that FD approximately preserves the norm of matrix vector products after sketch-

ing. Theorem 1 outlines the guarantees obtained by the returned summary $\mathbf{B} \in \mathbb{R}^{m \times d}$ of FD & *Robust Frequent Directions* (RFD). Huang (2018), show that RFD improves the accuracy of FD by a factor of 2. Both implementations are in Alg. A1, Appendix A.

Notation for Frequent Directions: we use $\Delta_k = \|\mathbf{A} - \mathbf{A}_k\|_F^2$ & $\alpha = 1/m-k$ to write the bounds for both FD & RFD (5).

Theorem 1 (Ghashami et al. (2016b); Huang (2018)). *Let $\mathbf{A} \in \mathbb{R}^{n \times d}$. The (Robust) Frequent Directions algorithm processes \mathbf{A} one row at a time, returns a matrix $\mathbf{B} \in \mathbb{R}^{m \times d}$ and a scalar δ such that for any unit vector $\mathbf{u} \in \mathbb{R}^d$:*

$$\|\mathbf{A}^\top \mathbf{A} - (\mathbf{B}^\top \mathbf{B} + \delta \mathbf{I}_d)\|_2 \leq \alpha' \Delta_k. \quad (5)$$

If $\mathbf{B} = \text{FD}(\mathbf{A})$, then $\delta = 0$ & $\alpha' = \alpha$. Else if $[\mathbf{B}, \delta] = \text{RFD}(\mathbf{A})$, δ is adaptively chosen and $\alpha' = \alpha/2$.

Modelling Assumptions. We assume that a dataset $\mathbf{A} \in \mathbb{R}^{n \times d}$ and targets $\mathbf{y} \in \mathbb{R}^n$ are given such that

$$\mathbf{y} = \mathbf{A}\mathbf{x}_0 + \boldsymbol{\varepsilon}. \quad (6)$$

For both statistical and optimization settings, we will assume that $n > d$ and the input data has $\text{rank}(\mathbf{A}) = d$ so that \mathbf{x}^* is uniquely defined.

Statistical setting. The noise $\boldsymbol{\varepsilon}$ is zero-mean, $\mathbb{E}(\boldsymbol{\varepsilon}) = \mathbf{0}_d$, and the covariance is $\mathbb{E}(\boldsymbol{\varepsilon}\boldsymbol{\varepsilon}^\top) = \sigma^2 \mathbf{I}_n$. For an estimate of the weights $\hat{\mathbf{x}}$, we are interested in

- bias($\hat{\mathbf{x}}$) = $\mathbb{E}(\hat{\mathbf{x}}) - \mathbf{x}_0$ & squared norm $\|\text{bias}(\hat{\mathbf{x}})\|_2^2$.
- Variance: $\text{var}(\hat{\mathbf{x}}) = (\hat{\mathbf{x}} - \mathbb{E}(\hat{\mathbf{x}}))(\hat{\mathbf{x}} - \mathbb{E}(\hat{\mathbf{x}}))^\top$ and its trace: $\text{trace}(\text{var}(\hat{\mathbf{x}}))$.
- Mean-square error (MSE): $\text{MSE}(\hat{\mathbf{x}}) = \mathbb{E}(\|\hat{\mathbf{x}} - \mathbf{x}_0\|_2^2)$ which by the bias-variance decomposition is $\text{MSE}(\hat{\mathbf{x}}) = \|\text{bias}(\hat{\mathbf{x}})\|_2^2 + \text{trace}(\text{var}(\hat{\mathbf{x}}))$.

All expectations are taken over the randomness in $\boldsymbol{\varepsilon}$.

Optimization setting. No assumptions on $\boldsymbol{\varepsilon}$ are made and it is assumed to be fixed. The notion of approximation we adopt is under the Euclidean norm: for an estimate $\hat{\mathbf{x}}$ how small can the *solution error* $\|\hat{\mathbf{x}} - \mathbf{x}^*\|_2$ be made.

Randomized Sketching typically require $\mathbf{S} \in \mathbb{R}^{m \times n}$ to obtain a $(1 \pm \rho)$ - ℓ_2 subspace embedding for \mathbf{A} (Woodruff, 2014) which preserves all $\text{rank}(\mathbf{A}) = d$ directions. There are many choices of \mathbf{S} which satisfy the necessary properties to compare to the bounds we present (Woodruff, 2014; Drineas & Mahoney, 2016). Prior work in both statistical & optimization perspectives, does not typically show a *strong* difference in accuracy based on how \mathbf{S} is generated (Wang et al., 2017; Pilanci & Wainwright, 2016; Cormode & Dickens, 2019). Thus, we focus only on the *Gaussian* and *Sparse Johnson-Lindenstrauss*

Transforms (SJLT) (Nelson & Nguyễn, 2013). The Gaussian is a high-quality sketch and is well-studied due to favorable properties such as rotational invariance (Lacotte & Pilanci, 2019; Pilanci & Wainwright, 2016) yet is slow to apply. Hence, we also test the SJLT, which has s nonzeros per column so is applied in time $O(\text{snnz}(\mathbf{A}))$ while also enjoying the same space bound. Details on constructing the sketches are found in Appendix E.

3 Statistical Properties of FDRR

Recall the linear model from Equation (6) which generates the data & assume $\gamma > 0$ is the regularisation parameter. Recall that $\mathbf{H}_\gamma = \mathbf{A}^\top \mathbf{A} + \gamma \mathbf{I}_d$, the exact solution is $\mathbf{x}^* = \mathbf{H}_\gamma^{-1} \mathbf{A}^\top \mathbf{y}$, $\hat{\mathbf{H}} = \mathbf{B}^\top \mathbf{B} + \gamma \mathbf{I}_d$ and FDRR returns $\hat{\mathbf{x}} = \hat{\mathbf{H}}^{-1} \mathbf{A}^\top \mathbf{y}$. Without sketching we have the following result for the optimal weights:

Lemma 1. *The optimal bias and variance terms are: $\text{bias}(\mathbf{x}^*) = -\gamma \mathbf{H}_\gamma^{-1} \mathbf{x}_0$ and $\text{var}(\mathbf{x}^*) = \sigma^2 \mathbf{H}_\gamma^{-1} \mathbf{A}^\top \mathbf{A} \mathbf{H}_\gamma^{-1}$*

The proof is given in Appendix B. Now, the task is to understand the extent to which approximating the weights through FDRR distorts the behaviour expressed in Lemma 1. To that end, we have the following lemma which expresses both the bias and variance of the weights $\hat{\mathbf{x}}$ found from solving FDRR.

Lemma 2 (FDRR bias and variance). *$\text{bias}(\hat{\mathbf{x}}) = (\hat{\mathbf{H}}^{-1} \mathbf{A}^\top \mathbf{A} - \mathbf{I}_d) \mathbf{x}_0$ and $\text{var}(\hat{\mathbf{x}}) = \sigma^2 \hat{\mathbf{H}}^{-1} \mathbf{A}^\top \mathbf{A} \hat{\mathbf{H}}^{-1}$.*

With this understanding, the next task is to relate these expressions to the corresponding terms achieved by \mathbf{x}^* as expressed in Lemma 1.

Observe that we may write $\text{bias}(\hat{\mathbf{x}})$ as $\text{bias}(\hat{\mathbf{x}}) = (\hat{\mathbf{H}}^{-1} \mathbf{A}^\top \mathbf{A} - \mathbf{I}_d) \mathbf{H}_\gamma \mathbf{H}_\gamma^{-1} \mathbf{x}_0$. This manipulation is useful as $\text{bias}(\mathbf{x}^*) = -\gamma \mathbf{H}_\gamma^{-1} \mathbf{x}_0$. Hence, if we can control the smallest and largest eigenvalues of $\mathbf{M} = (\hat{\mathbf{H}}^{-1} \mathbf{A}^\top \mathbf{A} - \mathbf{I}_d) \mathbf{H}_\gamma$ then we should be able to relate $\|\text{bias}(\hat{\mathbf{x}})\|_2^2$ to $\|\text{bias}(\mathbf{x}^*)\|_2^2$. This is exactly how our proof proceeds as we establish the following

Lemma 3. *Let $\gamma' = \gamma - \alpha \Delta_k > 0$. If $\mathbf{M} = (\hat{\mathbf{H}}^{-1} \mathbf{A}^\top \mathbf{A} - \mathbf{I}_d) \mathbf{H}_\gamma$, then $\lambda_{\max}(\mathbf{M}) \leq \gamma^2 / \gamma'$ & $\lambda_{\min}(\mathbf{M}) \geq \gamma'$*

Given that $\|\mathbf{M}\mathbf{u}\|_2 \in [\lambda_{\min}(\mathbf{M})\|\mathbf{u}\|_2, \lambda_{\max}(\mathbf{M})\|\mathbf{u}\|_2]$ we can take $\mathbf{u} = \mathbf{H}_\gamma^{-1} \mathbf{x}_0$ combined with Lemma 3 to establish: $\|\text{bias}(\hat{\mathbf{x}})\|_2^2 \in \left[\gamma'^2 \|\text{bias}(\mathbf{x}^*)\|_2^2, \frac{\gamma^4}{\gamma'^2} \|\text{bias}(\mathbf{x}^*)\|_2^2 \right]$. Finally, provided that the parameters of the FD sketch are appropriately set compared to the regularization γ , $\|\text{bias}(\hat{\mathbf{x}})\|_2^2$ can be shown to be within accurate relative-error bounds of $\|\text{bias}(\mathbf{x}^*)\|_2^2$.

Theorem 2. *Let $\mathbf{B} = \text{FD}(\mathbf{A}) \in \mathbb{R}^{m \times d}$ and let $\theta \in$*

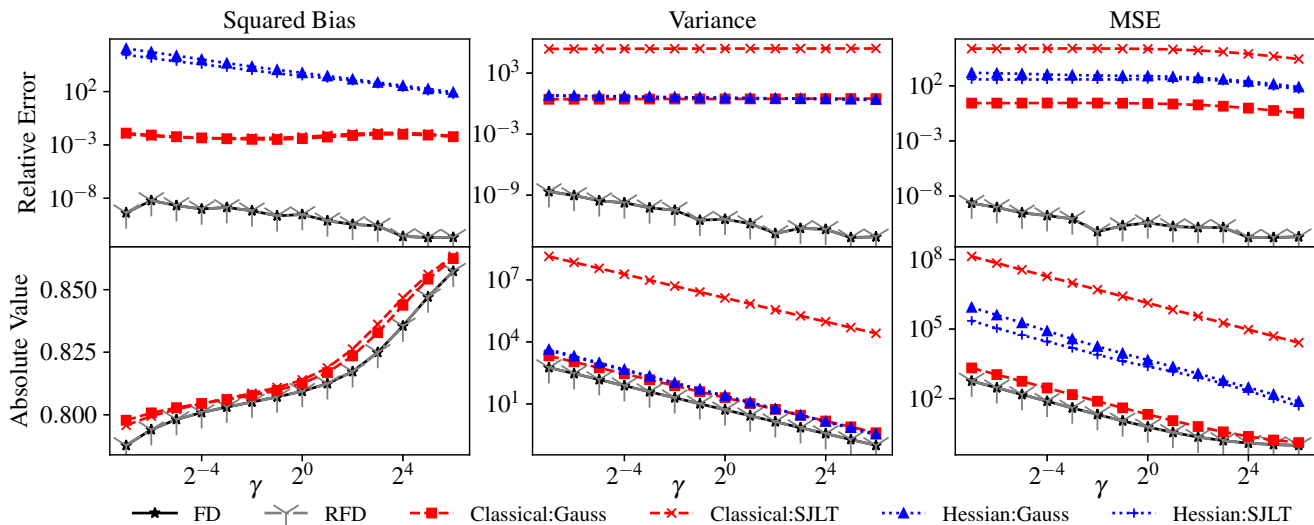


Figure 1: *Relative error* (top) and reported *absolute value* (bottom) of the 3 metrics $\|\text{bias}(\hat{\mathbf{x}})\|^2, \text{trace}(\text{var}(\hat{\mathbf{x}})), \text{MSE}(\hat{\mathbf{x}})$ plotted against γ . The instance has effective dimension $R_1 = \lfloor 0.15d + 0.5 \rfloor$. The deterministic methods dominate the randomized methods in all 3 metrics. *Hessian Sketch* has high error in estimating $\|\text{bias}(\mathbf{x}^*)\|_2^2$ so is omitted from the bottom left panel.

$(0, 1)$ be a parameter. If $m = \|\mathbf{A} - \mathbf{A}_k\|_F^2 / (1 - \sqrt{1 - \theta})\gamma + k$, then

$$\|\text{bias}(\hat{\mathbf{x}})\|_2^2 \in \left[(1 - \theta) \|\text{bias}(\mathbf{x}^*)\|_2^2, \frac{1}{1 - \theta} \|\text{bias}(\mathbf{x}^*)\|_2^2 \right]$$

Dealing with the variance terms is slightly simpler than the bias terms. This is thanks to the fact that, $\hat{\mathbf{H}} = \mathbf{B}^\top \mathbf{B} + \gamma \mathbf{I}_d$ is symmetric positive definite so we can exploit the *Löwner* ordering over such matrices. Expressing the variance of the weights $\hat{\mathbf{x}}$ is simple and follows the same approach as for the optimal weights \mathbf{x}^* . Subsequently, we need only invoke standard properties of the Löwner ordering to establish bounds on $\text{var}(\hat{\mathbf{x}})$ compared to $\text{var}(\mathbf{x}^*)$. One final nice property of the Löwner ordering is that the trace also respects the precedence. That is, if $\mathbf{X} \preceq \mathbf{Y}$ then $\text{trace}(\mathbf{X}) \leq \text{trace}(\mathbf{Y})$. This is the final piece to obtain:

Theorem 3. *Under the same assumptions as Theorem 2,* $\text{trace}(\text{var}(\hat{\mathbf{x}})) \in \left[(1 - \theta) \text{trace}(\text{var}(\mathbf{x}^*)), \frac{1}{1 - \theta} \text{trace}(\text{var}(\mathbf{x}^*)) \right]$.

Theorems 2 & 3 immediately entail the same guarantee on the MSE. Therefore;

Theorem 4. *Under the same assumptions as Theorem 2,* $(1 - \theta) \text{MSE}(\mathbf{x}^*) \leq \text{MSE}(\hat{\mathbf{x}}) \leq \frac{1}{1 - \theta} \text{MSE}(\mathbf{x}^*)$.

All proofs for this section are in Appendix B.2, including the extension to obtain a tighter approximation guarantee with RFD (App. B.3).

3.1 Experimental Evaluation

Competing Methods. We compare the *deterministic methods* (Robust) Frequent Directions Ridge Regression (R)FDRR against the randomized *Classical*

and *Hessian* sketches (Equations (3), (4)). The two methods for generating \mathbf{S} are *Gaussian* and SJLT with a sparsity of $s = 10$. We refer to the competing methods by SketchModel:SketchType, e.g. Classical:Gaussian.

Data Generation. We test on synthetic data generated in a similar fashion to Shi & Phillips (2020). The data size is $(n, d) = (2^{10}, 2^9)$ and has *effective rank* $R = \lfloor rd + 0.5 \rfloor$ for $r \in (0, 1)$. This ensures that most of the energy is concentrated on roughly the top r -fraction of the directions and is also used to fix the sparsity of the underlying (and unobserved) ground truth vector \mathbf{x}_0 which generates the data. We take $\mathbf{y} = \mathbf{A}\mathbf{x}_0 + \varepsilon$ with every $\varepsilon_i \sim \mathcal{N}(0, 2^2)$. Further details for generating the data are in Appendix E.

Experimental Setup. We choose $R_1 = \lfloor 0.15d + 0.5 \rfloor$ and $R_2 = \lfloor 0.25d + 0.5 \rfloor$ so that R_2 is of higher effective rank. This parameter setting is used to generate the linear model as described above. Then we plot the analytical expressions for bias, variance and MSE for (R)FDRR (Sec. 3) and the randomized methods. We set $m = 256$ and vary $\gamma \in \{2^{-8}, \dots, 2^6\}$ for all methods. The random methods are tested 10 times with the median results being reported. Only one trial is necessary for the deterministic methods. For the three metrics there is an optimal value u^* which is a function of \mathbf{x}^* estimated by \hat{u} , a function of $\hat{\mathbf{x}}$. We measure the *relative error* $|\hat{u} - u^*|/u^*$ and the *absolute value* of the estimate \hat{u} . Results are reported in Figure 1.

Findings: R_1 . Across all 3 metrics, both deter-

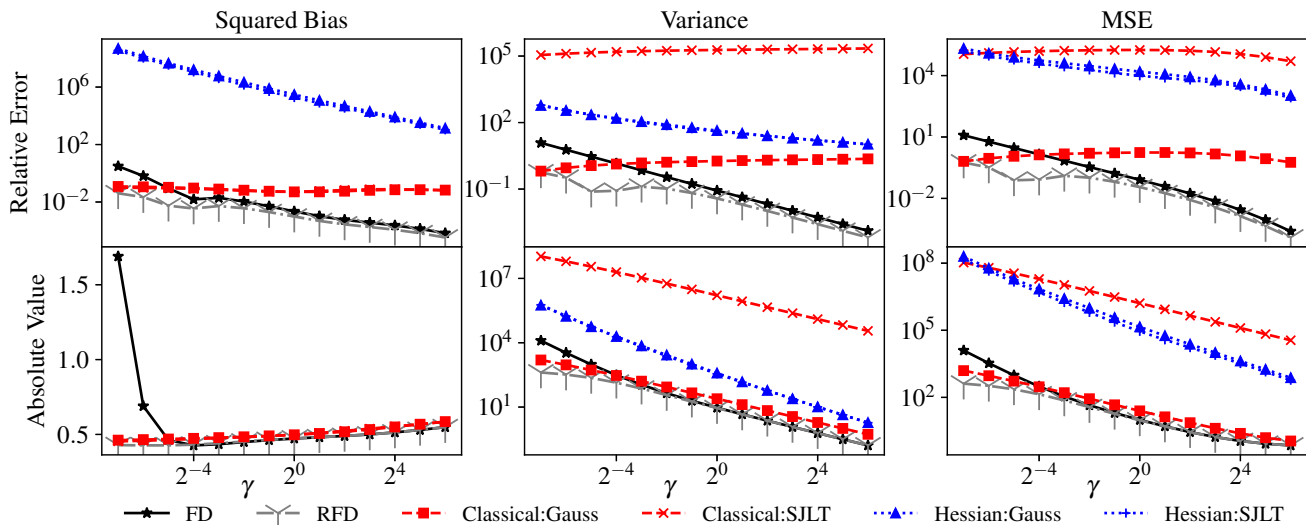


Figure 2: The three metrics vs γ for $R_2 = [0.25d + 0.5]$. FDRR performs worse than RFDRR at small values of γ but then begins to improve. Holistically, RFDRR dominates; FDRR is next best for large enough γ ; the randomized methods each have their deficiencies in bias, variance, or scalability (Gaussian sketch).

ministic methods dominate the randomized methods. At this projection dimension m , RFDRR is marginally better than FDRR, but the difference in performance negligible. The relative error of all three metrics is consistently many orders of magnitude better than randomized methods. For the bias, both Classical:Gaussian and Classical:SJLT method are the most competitive; in absolute terms they are not too far from $\|\text{bias}(\mathbf{x}^*)\|^2$ yet their relative error is much weaker than the deterministic methods. The Classical:Gaussian sketch appears most consistently competitive to (R)FDRR, however, this is not scalable for large data streams. Classical:SJLT appears competitive for bias but has the worst variance. On the other hand, both Hessian sketch methods substantially overestimate the bias yet their variance is sandwiched between the variance of Classical:Gaussian and Classical:SJLT. In the Hessian sketch model, there is little change observed between using Gaussian or SJLT.

Findings: R_2 . The sketch dimension has been maintained at $m = 256$. At this effective dimension we see differences in the deterministic methods as shown in Figure 2. The relative errors are higher than in Figure 1 due to the increased complexity of the ridge regression problem ($R_2 > R_1$). RFDRR remains consistently the best performing sketch across all 3 metrics. In relative error, FDRR performs up to roughly 2 orders of magnitude worse than RFDRR and roughly 1 order of magnitude worse than Classical:Gaussian in bias and variance up to $\gamma \leq 2^{-4}$. However, for $\gamma > 2^{-4}$ FDRR begins to perform similarly to RFDRR in both bias and variance. For the randomized sketches, Clas-

sical:Gaussian again looks competitive for small γ , yet once roughly $\gamma > 2^{-4}$, there appears to be no improvement in relative error and its utility appears to wane, in contrast to (R)FDRR. As in Figure 1, we observe the same deficiencies with Classical:SJLT and both Hessian sketch methods.

Summary. Across all 3 metrics and in both the low (R_1) and higher (R_2) effective rank regression problems, RFDRR is the standout sketch method. For less complex problems (R_1), FDRR is competitive with RFDRR, however when the complexity of the problem is increased (R_2), this behaviour becomes dependent on the regularisation. For the randomized methods, Classical:Gaussian is the most competitive with the deterministic methods, but this is fraught with scalability issues as it takes $O(nd^2)$ time to generate **SA**. When more scalable sketches are used instead of the Gaussian, or the Hessian Sketch approach is used, there is noticeable performance degradation.

4 Iterative Frequent Directions Ridge Regression

Shi & Phillips (2020) guarantee a ‘mid-precision’ approximation $\hat{\mathbf{x}}$ to \mathbf{x}^* . By that we mean, maintaining $m \geq k + \|\mathbf{A} - \mathbf{A}_k\|_F^2 / \gamma \zeta$ rows in the sketch ensures error $\|\hat{\mathbf{x}} - \mathbf{x}^*\|_2 \leq \zeta \|\mathbf{x}^*\|_2$. Thus the sketch grows according to $O(1/\zeta)$ for ζ accuracy; this is fine if ζ is not too small, but if an application requires the error of $\|\hat{\mathbf{x}} - \mathbf{x}^*\|_2$ to be very small (say 10^{-8} or less), then this behaviour is not ideal.

The estimate $\hat{\mathbf{x}}$ can be refined to better approximate \mathbf{x}^* through iterative gradient steps at the

Algorithm 1: Iterative Frequent Directions Ridge Regression iFDRR

Input: Data $\mathbf{A} \in \mathbb{R}^{n \times d}$, targets $\mathbf{b} \in \mathbb{R}^n$,
 regularisation $\gamma > 0$, sketch size m ,
 num. iterations $t \geq 1$, Method
 $\text{Sk} \in \{\text{FD}, \text{RFD}\}$

Output: Weights $\hat{\mathbf{x}} \in \mathbb{R}^d$

- 1 $\mathbf{B}, \rho = \text{Sk}(\mathbf{A}) \quad \triangleright \rho = 0$ if $\text{Sk} = \text{FD}$ else is
 nonzero
 - 2 $\hat{\mathbf{H}} = (\mathbf{B}^\top \mathbf{B} + (\gamma + \rho)\mathbf{I}_d)^{-1}$, $\mathbf{c} = \mathbf{A}^\top \mathbf{b}$, $\mathbf{x}^{(0)} = \mathbf{0}_d$
 - 3 **for** $i = 1 : t$ **do**
 - 4 $\mathbf{x}^{(i+1)} = \mathbf{x}^{(i)} - \hat{\mathbf{H}}^{-1} \mathbf{A}^\top (\mathbf{A} \mathbf{x}^{(i)} - \mathbf{b})$
 - 5 **end**
 - 6 $\hat{\mathbf{x}} = \mathbf{x}^{(t)}$
-

cost of further passes over the data. Our proposal (Alg. 1) is a Newton-type algorithm that exploits scalable approximation to the Hessian \mathbf{H}_γ . Our approach here is reminiscent of many other iterative sketching algorithms (Pilanci & Wainwright, 2016; Chowdhury et al., 2018). In common with both of them is that our summary \mathbf{B} has $o(d)$ rows, a substantial saving over explicitly using the $d \times d$ size Hessian matrix. The structure of $\hat{\mathbf{H}}$ avoids the $O(d^3)$ time cost for inversion due to the trick of Shi & Phillips (2020) or Woodbury’s Identity.

To prove correctness of Algorithm 1 we closely follow typical proofs for gradient descent-type algorithms. A key property we need is that the gradient of $f(\mathbf{x})$ is $\nabla f(\mathbf{x}) = \mathbf{H}_\gamma(\mathbf{x} - \mathbf{x}^*)$ (Lemma 16, Appendix C). Then we are able to analyse the sequence of iterates relative to their distance from \mathbf{x}^* . Crucially, we obtain:

$$\begin{aligned} \mathbf{x}^{(t+1)} &= \mathbf{x}^{(t)} - \hat{\mathbf{H}}^{-1} \nabla f(\mathbf{x}^{(t)}) \\ &= \mathbf{x}^{(t)} - \hat{\mathbf{H}}^{-1} \mathbf{H}_\gamma(\mathbf{x}^{(t)} - \mathbf{x}^*). \end{aligned} \quad (7)$$

Hence, $\mathbf{x}^{(t+1)} - \mathbf{x}^* = (\mathbf{I}_d - \hat{\mathbf{H}}^{-1} \mathbf{H}_\gamma)(\mathbf{x}^{(t)} - \mathbf{x}^*)$.

Therefore, to show convergence it is enough for us to establish the following lemma:

Lemma 4. *If $\gamma > 2\|\mathbf{A} - \mathbf{A}_k\|_F^2/(m - k)$, then $\|\mathbf{I}_d - \hat{\mathbf{H}}^{-1} \mathbf{H}_\gamma\|_2 < 1$*

Remark 1. *We claim that the assumption on γ in Lemma 4 is valid. Since $m - k \geq 1$ the assumption asks that γ is some fraction of the tail or residual of the mass. As ridge regression is intended to apply in the high-dimensional setting with much redundancy in the feature space, it is typical to assume that the regularization exceeds the tail in such a fashion.*

The proof of Lemma 4 is presented in Appendix C. It amounts to manipulating the FD guarantee of

Theorem 1 alongside properties of the Löwner ordering. The starting point is to analyse the spectrum of $\mathbf{I}_d - \hat{\mathbf{H}}^{-1} \mathbf{H}_\gamma$. By matrix similarity we instead analyse $\mathbf{I}_d - \hat{\mathbf{H}}^{-1/2} \mathbf{H}_\gamma \hat{\mathbf{H}}^{-1/2}$ but specifically need the extremal eigenvalues of the auxiliary matrix $\mathbf{E} = \hat{\mathbf{H}}^{-1/2} (\mathbf{A}^\top \mathbf{A} + \gamma \mathbf{I}_d) \hat{\mathbf{H}}^{-1/2}$.

Crucially, we show that all $\lambda_i(\mathbf{E}) \in [1, \frac{1}{1-q}]$ where $q = \frac{\|\mathbf{A} - \mathbf{A}_k\|_F^2}{(m-k)\gamma}$. This implies that the largest distortion $|1 - \lambda_i(\mathbf{E})|$ occurs at $|1 - \frac{1}{1-q}|$. Recall that for convergence we required $\|\mathbf{I}_d - \hat{\mathbf{H}}^{-1} \mathbf{H}_\gamma\|_2 < 1$ which is satisfied provided $|1 - \frac{1}{1-q}| < 1$. Hence, we need $q < 1/2$ which is true by the assumption of Lemma 4. Finally, we have the convergence theorem which follows by combining all of the above pieces. Details can be found in Appendix C.

Theorem 5. *Let $b \in (0, 1/2)$, $\alpha = 1/m-k$, $\Delta_k = \|\mathbf{A} - \mathbf{A}_k\|_F^2$ and suppose that $\alpha\Delta_k = b\gamma$. The iterative sketch algorithm for regression with Frequent Directions satisfies $\|\mathbf{x}^{(t+1)} - \mathbf{x}^*\|_2 \leq (b/(1-b))^{t+1} \|\mathbf{x}^*\|_2$*

Theorem 5 demonstrates that convergence is governed by an interplay between the regularisation parameter and the tail of mass. Let $\beta = \frac{b}{1-b}$ so that $\beta = \alpha\Delta_k/(\gamma - \alpha\Delta_k)$. When β is smaller, decay is faster. Hence, we can understand the tradeoff between regularisation and sketch accuracy necessary for convergence. Decreasing β can be achieved by increasing γ or by reducing $\alpha\Delta_k$. The former regularises the data more (less importance is placed on the observed data) while the latter is equivalent to choosing a greater sketch size. For example, taking $b = 1/4$, Theorem 5 yields $\gamma = 4\alpha\Delta_k$ so $\beta = 1/3$ & the error decreases by (at worst) a factor of 3 each iteration.

Remark 2. *Although $\|\mathbf{A} - \mathbf{A}_k\|_F^2$ may not be known (or cannot be estimated) in advance, setting $k = 0$ amounts to taking $b = \frac{\|\mathbf{A}\|_F^2}{m\gamma}$, but this may be too pessimistic in practice: $\|\mathbf{A}\|_F^2$ can be maintained in small space while observing the stream.*

4.1 Improving Performance with RFD

One downside of Theorem 5 is the fairly stringent assumption $2\alpha\Delta_k < \gamma$. While this is valid, it would be preferable to weaken this constraint. Indeed, this is possible due to the improved sketch quality of Robust Frequent Directions. Theorem 6 weakens the assumption of $2\alpha\Delta_k < \gamma$ to ask for $\alpha\Delta_k < \gamma$, while simultaneously improving the rate of convergence from $b/1-b$ to $b/2-b$. Recalling the previous example of taking $b = 1/4$, this is an improvement from $\beta = 1/3$ by Theorem 5 to $\beta = 1/7$.

Theorem 6. *Let $b \in (0, 1)$ and suppose that $\alpha\Delta_k = b\gamma$. The iterative sketch algorithm for regression with Robust Frequent Directions satisfies $\|\mathbf{x}^{(t+1)} - \mathbf{x}^*\|_2 \leq$*

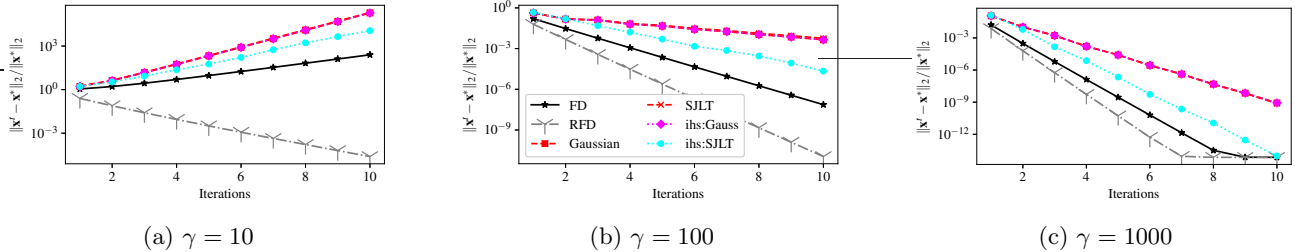


Figure 3: Algorithm 1 on W8A dataset for $\gamma = 10, 100, 1000$. Our approaches, FD and RFD outperform the randomized methods. The nearest competitor is IHS:SJLT which requires a new sketch for every gradient step. Our method requires only a single sketch.

$$(b/2-b)^{t+1} \|\mathbf{x}^*\|_2.$$

Due to the theory established for Theorem 5, we can essentially repeat the proof, adjusting for the necessary constants which arise due to using the RFD sketch $\mathbf{B}^\top \mathbf{B} + \delta \mathbf{I}_d$ instead of $\mathbf{B}^\top \mathbf{B}$.

4.2 Experimental Evaluation.

Setup. All methods were tested over 10 iterations using $m = 256$ rows to generate the sketch. We generate approximations to \mathbf{H}_γ using the *deterministic methods* FD and RFD. We also test Algorithm 1 with *randomized methods*: the first is to generate a new sketch $\mathbf{S}^{(t)}$ for every iteration t and set $\tilde{\mathbf{H}}^{(t)} = \mathbf{A}^\top \mathbf{S}^{(t)\top} \mathbf{S}^{(t)} \mathbf{A} + \gamma \mathbf{I}_d$. This is exactly the *Iterative Hessian Sketch* (IHS) technique of Pilanci & Wainwright (2016). The second generates a *single* approximation $\tilde{\mathbf{H}}$ to \mathbf{H}_γ and is a modification of IHS requiring only one sketch (Lacotte & Pilanci, 2019). Technically, using a single random sketch requires the tuning of a step size parameter but for comparison to our method we set the step size to 1. We choose \mathbf{S} to be Gaussian or an SJLT and refer to the randomized approaches as IHS:Gaussian, IHS:SJLT for IHS methods or Single:Gaussian & Single:SJLT when only a single sketch is used.

Datasets. We tested on the YearPredictionsMSD, ForestCover (Asuncion & Newman, 2007) & W8A datasets (Chang & Lin, 2011). We take the first $n = 10^5$ samples; these datasets are low dimensionality so we expand the feature space using Random Fourier Features (Rahimi & Recht, 2008) into $d = 1024$ using the `RFBFSampler` with default settings from `scikit-learn` (Pedregosa et al., 2011).

Findings. We include the results for the W8A datasets in Figure 3. Since the behaviour is consistent across all three datasets, we defer the plots for YearPredictions and ForestCover datasets to Appendix C.2. We found that in line with Theorems 5 and 6, convergence was easier for all methods when γ was increased. When $\gamma = 10$ (the smallest value), all methods except for RFD diverged. When $\gamma = 100$, all

methods began to descend towards the optimum. At any fixed number of iterations the RFD sketch performed best. After 10 iterations RFD achieved error better than 10^{-10} , followed secondly by FD which achieved error of approximately 10^{-7} .

Next best was the IHS:SJLT, this is interesting for two reasons, firstly, the deterministic methods performed better than all randomized methods, and secondly, because the deterministic methods use only a *single* sketch, whereas the best randomized methods uses a *new sketch* for every gradient step! It appears that there is roughly a 1 – 2 order of magnitude difference between FD and IHS:SJLT. This relative difference is slightly less than the difference between using RFD and FD. The methods Single:Gaussian, Single:SJLT and IHS:Gaussian all perform poorly at this projection dimension of $m = 256$. When we increase γ to 1000, all methods begin to approach the optimum more rapidly than $\gamma = 10, 100$, but again RFD is the stand out winner. The ordering between the sketch methods established when $\gamma = 10, 100$ is repeated at $\gamma = 1000$ and similarly, this behaviour is reflected on all the datasets we tested.

In summary, if one requires a high-accuracy solution to the ridge regression problem, Algorithm 1 should be employed with a single RFD sketch. On the examples we tried, this consistently outperformed using FD, a single sketch, or refreshed random projections.

5 Conclusion

We have shown that FD and RFD can be analysed from the statistical perspective for sketched regression. Using properties of the sketch we have demonstrated that FDRR and RFDRR preserves bias, variance and MSE over the weights up to constant factor relative error. Similarly, we have shown that both FD and RFD can be employed in the iterated regression model to obtain a highly accurate solution. In both examples we have shown that FD performs better than widely-used random projections. However, from a practical

perspective, RFD performs the best in both the statistical and optimization settings.

Acknowledgments. CD would like to thank Lee Rhodes, Jon Malkin, Alex Saydakov, Graham Cormode,ang for useful discussions and feedback in the preparation of this work. The work of CD is supported by European Research Council grant ERC-2014-CoG 647557.

References

- Agarwal, P. K., Cormode, G., Huang, Z., Phillips, J. M., Wei, Z., and Yi, K. Mergeable summaries. *ACM Transactions on Database Systems (TODS)*, 38(4):1–28, 2013.
- Asuncion, A. and Newman, D. Uci machine learning repository, 2007.
- Avron, H., Clarkson, K. L., and Woodruff, D. P. Sharper bounds for regularized data fitting. In *RANDOM*, 2017.
- Brand, M. Incremental singular value decomposition of uncertain data with missing values. In *European Conference on Computer Vision*, pp. 707–720. Springer, 2002.
- Chang, C.-C. and Lin, C.-J. Libsvm: A library for support vector machines. *ACM transactions on intelligent systems and technology (TIST)*, 2(3):1–27, 2011.
- Chowdhury, A., Yang, J., and Drineas, P. An iterative, sketching-based framework for ridge regression. In *International Conference on Machine Learning*, pp. 989–998, 2018.
- Clarkson, K. L. and Woodruff, D. P. Low-rank approximation and regression in input sparsity time. *Journal of the ACM (JACM)*, 63(6):1–45, 2017.
- Cohen, M. B., Nelson, J., and Woodruff, D. P. Optimal Approximate Matrix Product in Terms of Stable Rank. 55:11:1–11:14, 2016. ISSN 1868-8969. doi: 10.4230/LIPIcs.ICALP.2016.11. URL <http://drops.dagstuhl.de/opus/volltexte/2016/6278>.
- Cormode, G. and Dickens, C. Iterative hessian sketch in input sparsity time. In *Neurips Workshop: Beyond First-Order Optimization Methods in Machine Learning*, 2019.
- De Klerk, E. *Aspects of semidefinite programming: interior point algorithms and selected applications*, volume 65. Springer Science & Business Media, 2006.
- Drineas, P. and Mahoney, M. W. Randnla: randomized numerical linear algebra. *Communications of the ACM*, 59(6):80–90, 2016.
- Ghashami, M., Liberty, E., and Phillips, J. M. Efficient frequent directions algorithm for sparse matrices. In *Proceedings of the 22nd ACM SIGKDD International Conference on Knowledge Discovery and Data Mining*, pp. 845–854, 2016a.
- Ghashami, M., Liberty, E., Phillips, J. M., and Woodruff, D. P. Frequent directions: Simple and deterministic matrix sketching. *SIAM Journal on Computing*, 45(5):1762–1792, 2016b.
- Huang, Z. Near optimal frequent directions for sketching dense and sparse matrices. In *International Conference on Machine Learning*, pp. 2048–2057. PMLR, 2018.
- Lacotte, J. and Pilanci, M. Faster least squares optimization. *arXiv preprint arXiv:1911.02675*, 2019.
- Liberty, E. Simple and deterministic matrix sketching. In *Proceedings of the 19th ACM SIGKDD international conference on Knowledge discovery and data mining*, pp. 581–588, 2013.
- Luo, L., Chen, C., Zhang, Z., Li, W.-J., and Zhang, T. Robust frequent directions with application in online learning. *Journal of Machine Learning Research*, 20(45):1–41, 2019. URL <http://jmlr.org/papers/v20/17-773.html>.
- Nelson, J. and Nguyen, H. L. Osnap: Faster numerical linear algebra algorithms via sparser subspace embeddings. In *2013 IEEE 54th Annual Symposium on Foundations of Computer Science*, pp. 117–126. IEEE, 2013.
- Pedregosa, F., Varoquaux, G., Gramfort, A., Michel, V., Thirion, B., Grisel, O., Blondel, M., Prettenhofer, P., Weiss, R., Dubourg, V., et al. Scikit-learn: Machine learning in python. *the Journal of machine Learning research*, 12:2825–2830, 2011.
- Pilanci, M. and Wainwright, M. J. Randomized sketches of convex programs with sharp guarantees. *IEEE Transactions on Information Theory*, 61(9): 5096–5115, 2015.
- Pilanci, M. and Wainwright, M. J. Iterative hessian sketch: Fast and accurate solution approximation for constrained least-squares. *The Journal of Machine Learning Research*, 17(1):1842–1879, 2016.
- Rahimi, A. and Recht, B. Random features for large-scale kernel machines. In *Advances in neural information processing systems*, pp. 1177–1184, 2008.
- Shi, B. and Phillips, J. M. A deterministic streaming sketch for ridge regression. *arXiv preprint arXiv:2002.02013*, 2020.
- van Wieringen, W. N. Lecture notes on ridge regression. *arXiv preprint arXiv:1509.09169*, 2015.

Wang, S., Gittens, A., and Mahoney, M. W. Sketched ridge regression: Optimization perspective, statistical perspective, and model averaging. *The Journal of Machine Learning Research*, 18(1):8039–8088, 2017.

Woodruff, D. P. Sketching as a tool for numerical linear algebra. *Foundations and Trends® in Theoretical Computer Science*, 10(1–2):1–157, 2014. ISSN 1551-305X. doi: 10.1561/04000000060. URL <http://dx.doi.org/10.1561/04000000060>.

A Frequent Directions Properties

Algorithm A1: Frequent Directions (FD) and Robust Frequent Directions (RFD) (Ghashami et al., 2016a; Huang, 2018).

Input: Data $\mathbf{A} \in \mathbb{R}^{n \times d}$, sketch size m , method $\text{Sk} \in \{\text{FD}, \text{RFD}\}$
Output: $\mathbf{B} \in \mathbb{R}^{m \times d}$

- 1 Initialise $\mathbf{B} \leftarrow \mathbf{0}_{2m \times d}$
- 2 $\rho \leftarrow 0$ ▷ Parameter for RFD
- 3 **for** $i = 1 : n$ **do**
- 4 Insert row $\mathbf{A}[i, :]$ into all zeros row of \mathbf{B}
- 5 **if** \mathbf{B} has no zero rows **then**
- 6 $\mathbf{U}, \mathbf{\Sigma}, \mathbf{V}^\top = \text{SVD}(\mathbf{B})$
- 7 $\delta \leftarrow \sigma_m^2$
- 8 $\rho \leftarrow \rho + \delta/2$
- 9 $\mathbf{B} \leftarrow \sqrt{\max(\mathbf{\Sigma}^2 - \delta \mathbf{I}_m, 0)}$
- 10 **end**
- 11 **end**
- 12 **if** $\text{Sk} = \text{FD}$ **then**
- 13 $\rho \leftarrow 0$ ▷ $\rho = 0$ for standard FD
- 14 **end**
- 15 **return** \mathbf{B}, ρ

Algorithm A2: Frequent Directions Ridge Regression FDRR (Shi & Phillips, 2020)

Input: Data $\mathbf{A} \in \mathbb{R}^{n \times d}$, targets $\mathbf{b} \in \mathbb{R}^n$, hyperparameter $\gamma > 0$, sketch size m , method: $\text{Sk} \in \{\text{FD}, \text{RFD}\}$
Output: Weights $\hat{\mathbf{x}} \in \mathbb{R}^d$

- 1 $\mathbf{c} = \mathbf{A}^\top \mathbf{b}$
- 2 $\mathbf{B}, \rho = \text{Sk}(\mathbf{A})$ ▷ Call Alg. A1: $\rho = 0$ iff $\text{Sk} = \text{FD}$
- 3 $\hat{\mathbf{x}} = (\mathbf{B}^\top \mathbf{B} + (\gamma + \rho) \mathbf{I}_d)^{-1} \mathbf{c}$

We present the technical details for the results presented in the main body. Before proceeding to the proofs, we set up some notation and consequences of the Frequent Directions algorithm. For $k \geq 0$, let \mathbf{A}_k denote the optimal rank- k approximation to \mathbf{A} .

Theorem 7 (Ghashami et al. (2016b)). *Let $\mathbf{A} \in \mathbb{R}^{n \times d}$. The Frequent Directions algorithm processes \mathbf{A} one row at a time and returns a matrix $\mathbf{B} \in \mathbb{R}^{m \times d}$ such that for any unit vector $\mathbf{u} \in \mathbb{R}^d$:*

$$0 \leq \|\mathbf{A}\mathbf{u}\|_2^2 - \|\mathbf{B}\mathbf{u}\|_2^2 \leq \frac{\|\mathbf{A} - \mathbf{A}_k\|_F^2}{m - k}$$

We will repeatedly use the notation $\Delta_k = \|\mathbf{A} - \mathbf{A}_k\|_F^2$. An equivalent formulation of Theorem 7 is that in the Löwner ordering (see Section D for full definitions):

$$\mathbf{A}^\top \mathbf{A} - \frac{\Delta_k}{m - k} \mathbf{I}_d \preceq \mathbf{B}^\top \mathbf{B} \preceq \mathbf{A}^\top \mathbf{A}. \quad (8)$$

Since each of the above matrices is symmetric positive semidefinite we can exploit the Löwner ordering over such matrices (see Section D). This enables useful properties such as preservation of ordering under the following addition of $\gamma \mathbf{I}_d$. Let $\gamma' = \gamma - \Delta_k/m - k$:

$$\mathbf{A}^\top \mathbf{A} + \gamma' \mathbf{I}_d \preceq \mathbf{B}^\top \mathbf{B} + \gamma \mathbf{I}_d \preceq \mathbf{A}^\top \mathbf{A} + \gamma \mathbf{I}_d \quad (9)$$

Which we will denote

$$\mathbf{H}_{\gamma'} \preceq \hat{\mathbf{H}} \preceq \mathbf{H}_\gamma. \quad (10)$$

We will chiefly manipulate $\hat{\mathbf{H}} = \mathbf{B}^\top \mathbf{B} + \gamma \mathbf{I}_d$ being an approximation to $\mathbf{H}_{\gamma'} = \mathbf{A}^\top \mathbf{A} + \gamma \mathbf{I}_d$ which is bounded below by $\mathbf{H}_{\gamma'} = \mathbf{A}^\top \mathbf{A} + \gamma' \mathbf{I}_d$. The formulation of Equation (9) provides the foundation for us to analyse ridge regression with FD sketching. For instance, a basic but key result that underpins our bounds is:

Lemma 5. *Let $\mathbf{B} = \text{FD}(\mathbf{A})$ and let $\gamma > 0$ and $\gamma' = \gamma/m-k > 0$. Then $\gamma' \mathbf{I}_d \preceq \mathbf{B}^\top \mathbf{B} + \gamma \mathbf{I}_d - \mathbf{A}^\top \mathbf{A} \preceq \gamma \mathbf{I}_d$*

Proof. Let $\alpha = 1/m-k$. Theorem 7 establishes

$$\mathbf{A}^\top \mathbf{A} - \alpha \Delta_k \mathbf{I}_d \preceq \mathbf{B}^\top \mathbf{B} \preceq \mathbf{A}^\top \mathbf{A}.$$

Subtracting $\mathbf{A}^\top \mathbf{A}$ from (9) yields

$$-\alpha \Delta_k \mathbf{I}_d \preceq \mathbf{B}^\top \mathbf{B} - \mathbf{A}^\top \mathbf{A} \preceq \mathbf{0}_{d \times d}.$$

Adding $\gamma \mathbf{I}_d$ establishes the claim. \square

A.1 Relating \mathbf{H}_γ to $\mathbf{H}_{\gamma'}$

For $\gamma' = \gamma - s > 0$, we will prove Lemma 7 which relates $\mathbf{H}_{\gamma'}$ to \mathbf{H}_γ . This allows us to express the lower bound of (10) as

$$\frac{\gamma'}{\gamma} \mathbf{H}_\gamma \preceq \mathbf{H}_{\gamma'} \preceq \mathbf{H}_\gamma. \quad (11)$$

Note that by properties of the Löwner ordering over symmetric positive definite matrices, this also implies that the ordering of the eigenvalues is preserved:

$$\frac{\gamma'}{\gamma} \lambda_i(\mathbf{H}_\gamma) \preceq \lambda_i(\mathbf{H}_{\gamma'}) \preceq \lambda_i(\mathbf{H}_\gamma). \quad (12)$$

Before proving the claims which allow us to assert the above, we prove the following simple lemma:

Lemma 6. *If $x \geq 0$ and let $t > s > 0$, then*

$$\frac{t-s}{t}(x+t) \leq x+t-s < x+t.$$

Proof. The upper bound follows trivially since $t-s < t$. For the lower bound,

$$\begin{aligned} \frac{t-s}{t}(x+t) &= \frac{t-s}{t}x + (t-s) \\ &\leq x + (t-s) \end{aligned}$$

since $\frac{t-s}{t} < 1$ and $x \geq 0$. \square

Lemma 7. *Let $\mathbf{A} \in \mathbb{R}^{n \times d}$, $\gamma > 0$ and $\mathbf{H}_a = \mathbf{A}^\top \mathbf{A} + a \mathbf{I}_d$. If $\gamma' = \gamma - s > 0$, then*

$$\frac{\gamma'}{\gamma} \mathbf{H}_\gamma \preceq \mathbf{H}_{\gamma'} \preceq \mathbf{H}_\gamma.$$

Before proving Lemma 7 we focus on the diagonal part of the SVD. As we operate on a diagonal matrix, we can directly apply Lemma 6 to make the following assertion over the singular values of \mathbf{A} .

Lemma 8. *Let Σ^2 denote the diagonal matrix of singular values of an arbitrary input matrix $\mathbf{X} \in \mathbb{R}^{n \times d}$. Let $\gamma > 0$ be a regularization parameter from ridge regression which ensures that $0 \prec (\Sigma^2 + \gamma \mathbf{I}_d)$. Suppose that $\gamma' = \gamma - s$ and $\gamma' > 0$. Then:*

$$\frac{\gamma-s}{\gamma} (\Sigma^2 + \gamma \mathbf{I}_d) \preceq \Sigma^2 + \gamma' \mathbf{I}_d \preceq \Sigma^2 + \gamma \mathbf{I}_d. \quad (13)$$

Proof. Recall that $\Sigma^2 + a \mathbf{I}_d = \text{diag}(\sigma_i^2 + a)$ for arbitrary scalar $a \in \mathbb{R}$. Applying Lemma 6 on every $\sigma_i^2 + \gamma'$ ensures:

$$\frac{\gamma-s}{\gamma} (\sigma_i^2 + \gamma) \leq \sigma_i^2 + \gamma - s < \sigma_i^2 + \gamma \quad (14)$$

which proves the claim. \square

Proof of Lemma 7. This is immediate from introducing the orthogonal matrix \mathbf{V} from the SVD of \mathbf{A} , Lemma 8, and the property of the Löwner ordering that $\mathbf{CXC}^\top \preceq \mathbf{CYC}^\top$ if and only if $\mathbf{X} \preceq \mathbf{Y}$ ensure that, with $\mathbf{C} = \mathbf{V}$:

$$\frac{\gamma'}{\gamma} (\mathbf{V}\Sigma^2\mathbf{V}^\top + \gamma\mathbf{I}_d) \preceq \mathbf{V}\Sigma^2\mathbf{V}^\top + \gamma'\mathbf{I}_d \preceq \mathbf{V}\Sigma^2\mathbf{V}^\top + \gamma\mathbf{I}_d \quad (15)$$

that is;

$$\frac{\gamma'}{\gamma} (\mathbf{A}^\top \mathbf{A} + \gamma\mathbf{I}_d) \preceq \mathbf{A}^\top \mathbf{A} + \gamma'\mathbf{I}_d \preceq \mathbf{A}^\top \mathbf{A} + \gamma\mathbf{I}_d \quad (16)$$

□

Note that Lemma 7 admits the following overall relations when $\mathbf{B} = \text{FD}(\mathbf{A})$ (or $[\mathbf{C}, \delta] = \text{RFD}(\mathbf{A})$ so that $\mathbf{B} = \mathbf{C}^\top \mathbf{C} + \delta\mathbf{I}_d$):

$$\frac{\gamma'}{\gamma} (\mathbf{A}^\top \mathbf{A} + \gamma\mathbf{I}_d) \preceq \mathbf{A}^\top \mathbf{A} + \gamma'\mathbf{I}_d \preceq \mathbf{B}^\top \mathbf{B} + \gamma\mathbf{I}_d \preceq \mathbf{A}^\top \mathbf{A} + \gamma\mathbf{I}_d \quad (17)$$

$$(\mathbf{A}^\top \mathbf{A} + \gamma\mathbf{I}_d)^{-1} \preceq (\mathbf{A}^\top \mathbf{A} + \gamma'\mathbf{I}_d)^{-1} \preceq (\mathbf{B}^\top \mathbf{B} + \gamma\mathbf{I}_d)^{-1} \preceq \frac{\gamma}{\gamma'} (\mathbf{A}^\top \mathbf{A} + \gamma\mathbf{I}_d)^{-1} \quad (18)$$

B Statistical Perspectives

We present the technical results from Section 3. Recall from Equation (6) that we have the following model

$$\mathbf{y} = \mathbf{A}\mathbf{x}_0 + \boldsymbol{\varepsilon} \quad (19)$$

with $\mathbb{E}(\boldsymbol{\varepsilon}) = \mathbf{0}_d$ and variance $\mathbb{E}(\boldsymbol{\varepsilon}\boldsymbol{\varepsilon}^\top) = \sigma^2\mathbf{I}_n$. A consequence of this linear model is that

$$\mathbb{E}(\mathbf{y}) = \mathbf{A}\mathbf{x}_0, \quad (20)$$

a fact we repeatedly use.

B.1 Proof of Lemma 1

Recall that $\mathbf{x}^* = \mathbf{H}_\gamma^{-1}\mathbf{A}^\top \mathbf{y}$ is the optimal ridge regression solution. We have the following relations which express the bias, variance, and mean-square error (MSE) of \mathbf{x}^* *without* sketching. These have been previously established (see e.g. van Wieringen (2015)) yet we include them for completeness and consistency of notation.

Lemma 9. *The squared bias of the optimal weights \mathbf{x}^* is:*

$$\|\text{bias}(\mathbf{x}^*)\|_2^2 = \gamma^2 \|\mathbf{H}_\gamma^{-1}\mathbf{x}_0\|_2^2 \quad (21)$$

Proof.

$$\mathbb{E}(\mathbf{x}^*) = \mathbb{E}\left(\left(\mathbf{A}^\top \mathbf{A} + \gamma\mathbf{I}_d\right)^{-1} \mathbf{A}^\top \mathbf{y}\right) \quad (22)$$

$$= \left(\mathbf{A}^\top \mathbf{A} + \gamma\mathbf{I}_d\right)^{-1} \mathbf{A}^\top \mathbf{A}\mathbf{x}_0 \quad (23)$$

$$= \left(\mathbf{A}^\top \mathbf{A} + \gamma\mathbf{I}_d\right)^{-1} \left(\mathbf{A}^\top \mathbf{A} + \gamma\mathbf{I}_d - \gamma\mathbf{I}_d\right) \mathbf{x}_0 \quad (24)$$

$$= \mathbf{x}_0 - \gamma \left(\mathbf{A}^\top \mathbf{A} + \gamma\mathbf{I}_d\right)^{-1} \mathbf{x}_0. \quad (25)$$

Recalling that $\text{bias}(\mathbf{x}^*) = \mathbb{E}(\mathbf{x}^*) - \mathbf{x}_0$ and taking the squared norm recovers the stated result. □

For the variance we have the following:

Lemma 10. *The variance of the optimal weights is: $\text{var}(\mathbf{x}^*) = \sigma^2\mathbf{H}_\gamma^{-1}\mathbf{A}^\top \mathbf{A}\mathbf{H}_\gamma^{-1}$.*

Proof. Recalling from Equation (20) that $\mathbb{E}(\mathbf{y}) = \mathbf{A}\mathbf{x}_0$, we have

$$\text{var}(\mathbf{x}^*) = (\mathbf{x}^* - \mathbb{E}(\mathbf{x}^*)) (\mathbf{x}^* - \mathbb{E}(\mathbf{x}^*))^\top \quad (26)$$

$$= (\mathbf{H}_\gamma^{-1} \mathbf{A}^\top \mathbf{y} - \mathbf{H}_\gamma^{-1} \mathbf{A}^\top \mathbb{E}(\mathbf{y})) (\mathbf{H}_\gamma^{-1} \mathbf{A}^\top \mathbf{y} - \mathbf{H}_\gamma^{-1} \mathbf{A}^\top \mathbb{E}(\mathbf{y}))^\top \quad (27)$$

$$= \mathbf{H}_\gamma^{-1} \mathbf{A}^\top (\mathbf{y} - \mathbb{E}(\mathbf{y})) (\mathbf{y} - \mathbb{E}(\mathbf{y}))^\top \mathbf{A} \mathbf{H}_\gamma^{-1} \quad (28)$$

$$= \mathbf{H}_\gamma^{-1} \mathbf{A}^\top \text{var}(\mathbf{y}) \mathbf{A} \mathbf{H}_\gamma^{-1}. \quad (29)$$

Finally, we recognise that $\text{var}(\mathbf{y}) = \sigma^2 \mathbf{I}_n$ which establishes the claim. \square

Using these results for the bias and variance enables the following relationship for the *mean-squared error*. Recall that when \mathbf{x}_0 is the vector from the data-generation model, (19) then the mean-squared error of an estimator \mathbf{x} is defined as $\text{MSE}(\mathbf{x}) = \mathbb{E} \|\mathbf{x} - \mathbf{x}_0\|_2^2$.

Lemma 11. *The mean-squared error of \mathbf{x}^* is $\text{MSE}(\mathbf{x}^*) = \text{trace}(\text{var}(\mathbf{x}^*)) + \|\text{bias}(\mathbf{x}^*)\|_2^2$.*

Proof. We begin from the definition of $\text{MSE}(\mathbf{x}^*)$, adding and subtracting $\mathbb{E}(\mathbf{x}^*)$ in the norm term. Secondly, recall that from Lemma 9 $\text{bias}(\mathbf{x}^*) = \mathbb{E}(\mathbf{x}^*) - \mathbf{x}_0$. Then;

$$\begin{aligned} \text{MSE}(\mathbf{x}^*) &= \mathbb{E} \|\mathbf{x}^* - \mathbb{E}(\mathbf{x}^*) + \mathbb{E}(\mathbf{x}^*) - \mathbf{x}_0\|_2^2 \\ &= \mathbb{E} \|\mathbf{x}^* - \mathbb{E}(\mathbf{x}^*) + \text{bias}(\mathbf{x}^*)\|_2^2 \\ &= \mathbb{E} \|\mathbf{x}^* - \mathbb{E}(\mathbf{x}^*)\|_2^2 + \|\text{bias}(\mathbf{x}^*)\|_2^2 \\ &= \sum_{i=1}^d \mathbb{E}(\mathbf{x}_{\gamma(i)} - \mathbb{E}(\mathbf{x}^*)_i)^2 + \|\text{bias}(\mathbf{x}^*)\|_2^2 \\ &= \sum_{i=1}^d \text{var}(\mathbf{x}^*)_{ii} + \|\text{bias}(\mathbf{x}^*)\|_2^2 \\ &= \text{trace}(\text{var}(\mathbf{x}^*)) + \|\text{bias}(\mathbf{x}^*)\|_2^2 \end{aligned}$$

\square

Now that we have the properties on the optimal weights in hand, we can relate these to the estimates found from solving the sketched ridge problem.

B.2 Bias-Variance Tradeoff for FD Sketched Ridge Regression: Lemma 2 - Theorem 4

Recall that for sketched ridge regression the algorithm is roughly: (i) obtain an FD sketch $\mathbf{B} = \text{FD}(\mathbf{A})$; (ii) return $\hat{\mathbf{x}} = (\mathbf{B}^\top \mathbf{B} + \gamma \mathbf{I}_d)^{-1} \mathbf{A}^\top \mathbf{y}$. We will use the shorthand $\hat{\mathbf{H}} = \mathbf{B}^\top \mathbf{B} + \gamma \mathbf{I}_d$ (which is an approximation to \mathbf{H}_γ , although we suppress the γ notation for $\hat{\mathbf{H}}$). Our analysis to evaluate the bias and variance roughly follows the same lines as in the preceding section. However, we need to understand the spectral properties of the sketch \mathbf{B} .

Lemma 12. $\text{bias}(\hat{\mathbf{x}}) = (\hat{\mathbf{H}}^{-1} \mathbf{A}^\top \mathbf{A} - \mathbf{I}_d) \mathbf{x}_0$

Proof. Observe that $\mathbb{E}(\hat{\mathbf{x}}) = (\mathbf{B}^\top \mathbf{B} + \gamma \mathbf{I}_d)^{-1} \mathbf{A}^\top \mathbf{A} \mathbf{x}_0$. Adding and subtracting \mathbf{x}_0 yields the result. \square

The task is now to bound $\|\text{bias}(\hat{\mathbf{x}})\|_2^2$ in comparison to the optimal weights $\|\text{bias}(\mathbf{x}^*)\|_2^2$ found from solving unsketched problem. We need the following lemma which relates the distortion of a matrix-vector product to the extremal eigenvalues of the matrix.

Lemma 13 (Extremal distortion of vector norm). *Let $\mathbf{M} \in \mathbb{R}^{d \times d}$ be a symmetric positive definite matrix which has largest and smallest eigenvalues $\lambda_{\max}(\mathbf{M})$, $\lambda_{\min}(\mathbf{M})$, respectively. Let $\mathbf{u} \in \mathbb{R}^d$ be arbitrary. Then*

$$\lambda_{\min}(\mathbf{M}) \|\mathbf{u}\|_2 \leq \|\mathbf{M}\mathbf{u}\|_2 \leq \lambda_{\max}(\mathbf{M}) \|\mathbf{u}\|_2$$

Proof. Follows from eigendecomposition of \mathbf{M} . \square

In order to express $\text{bias}(\hat{\mathbf{x}})$ in terms of $\text{bias}(\mathbf{x}^*)$ we multiply by $\mathbf{H}_\gamma \mathbf{H}_\gamma^{-1}$. That is

$$\text{bias}(\hat{\mathbf{x}}) = (\tilde{\mathbf{H}}^{-1} \mathbf{A}^\top \mathbf{A} - \mathbf{I}_d) \mathbf{H}_\gamma \cdot \mathbf{H}_\gamma^{-1} \mathbf{x}_0. \quad (30)$$

Now define the matrix $\mathbf{M} = (\tilde{\mathbf{H}}^{-1} \mathbf{A}^\top \mathbf{A} - \mathbf{I}_d) \mathbf{H}_\gamma$. Provided that we can control the spectrum of \mathbf{M} , then it will be possible to invoke Lemma 13: this is demonstrated in the subsequent result.

Lemma 14. *Let $\mathbf{M} = (\hat{\mathbf{H}}^{-1} \mathbf{A}^\top \mathbf{A} - \mathbf{I}_d) \mathbf{H}_\gamma$. Then $\lambda_{\max}(\mathbf{M}) \leq \gamma^2/\gamma'$ and $\lambda_{\min}(\mathbf{M}) \geq \gamma'$*

Proof. We will multiply \mathbf{M} by -1 which has the effect of only changing the signs but not the magnitude of the eigenvalues. Then apply the extremal value condition of the generalised Rayleigh quotient (see Section D):

$$\lambda_{\max}(\mathbf{M}) = \max_{\mathbf{u}: \|\mathbf{u}\|_2=1} |\mathbf{u}^\top (\mathbf{I}_d - \hat{\mathbf{H}}^{-1} \mathbf{A}^\top \mathbf{A}) \mathbf{H}_\gamma \mathbf{u}|$$

from which we can pass the inverse into the denominator (see e.g. Lemma 1 Shi & Phillips (2020)):

$$\lambda_{\max}(\mathbf{M}) = \max_{\mathbf{u}: \|\mathbf{u}\|_2=1} \left| \frac{\mathbf{u}^\top (\hat{\mathbf{H}} - \mathbf{A}^\top \mathbf{A}) \mathbf{H}_\gamma \mathbf{u}}{\mathbf{u}^\top \hat{\mathbf{H}} \mathbf{u}} \right|.$$

Now apply the variable change $\mathbf{z} = \mathbf{H}_\gamma^{1/2} \mathbf{u}$, noting that since \mathbf{H}_γ is symmetric positive definite it has symmetric positive definite square roots (Section D). Thus:

$$\lambda_{\max}(\mathbf{M}) = \max_{\mathbf{z}} \left| \frac{\mathbf{z}^\top \mathbf{H}_\gamma^{-1/2} (\tilde{\mathbf{H}} - \mathbf{A}^\top \mathbf{A}) \mathbf{H}_\gamma^{1/2} \mathbf{z}}{\mathbf{z}^\top \mathbf{H}_\gamma^{-1/2} \hat{\mathbf{H}} \mathbf{H}_\gamma^{1/2} \mathbf{z}} \right|. \quad (31)$$

To bound the numerator we combat the central term by applying Lemma 5 which shows $\tilde{\mathbf{H}} - \mathbf{A}^\top \mathbf{A} \preceq \gamma \mathbf{I}_d$. Thus;

$$\lambda_{\max}(\mathbf{M}) \leq \gamma \max_{\mathbf{z}} \left| \frac{\mathbf{z}^\top \mathbf{H}_\gamma^{-1/2} \mathbf{H}_\gamma^{1/2} \mathbf{z}}{\mathbf{z}^\top \mathbf{H}_\gamma^{-1/2} \hat{\mathbf{H}} \mathbf{H}_\gamma^{1/2} \mathbf{z}} \right|.$$

Reverting back to the original coordinates over \mathbf{u} this is:

$$\lambda_{\max}(\mathbf{M}) \leq \gamma \max_{\mathbf{u}: \|\mathbf{u}\|_2=1} \left| \frac{\mathbf{u}^\top \mathbf{H}_\gamma \mathbf{u}}{\mathbf{u}^\top \hat{\mathbf{H}} \mathbf{u}} \right|. \quad (32)$$

Now it remains to lower bound the spectrum of the denominator term in $\hat{\mathbf{H}}$. Again, due to FD we have $\hat{\mathbf{H}} \succeq \mathbf{H}_{\gamma'}$ and Lemma 7, we know $\gamma'/\gamma \mathbf{H}_\gamma \preceq \mathbf{H}_{\gamma'} \preceq \hat{\mathbf{H}}$. Thus, we have $\lambda_{\min}(\hat{\mathbf{H}}) \lambda_{\min}(\mathbf{H}_{\gamma'}) \geq (\gamma'/\gamma) \lambda_{\min}(\mathbf{H}_\gamma)$. Plugging this into (32) yields $\lambda_{\max}(\mathbf{M}) \leq \gamma^2/\gamma'$, as required.

For the lower bound we follow essentially the same approach but need to lower bound the $\hat{\mathbf{H}} - \mathbf{A}^\top \mathbf{A}$ in (31), again using Lemma 5 to show $\lambda_{\min}(\hat{\mathbf{H}} - \mathbf{A}^\top \mathbf{A}) \geq \gamma'$. For the denominator, we use Equation (17) which reduces the absolute value term to 1. Finally, the claim follows from Lemma 13. \square

We are now in a position to provide constant factor approximation bounds for the bias of the estimate returned by FD sketched ridge regression.

Theorem 8. *Let $\mathbf{B} = \text{FD}(\mathbf{A}) \in \mathbb{R}^{m \times d}$. Let $\theta \in (0, 1)$ be a parameter and set $c^2 = 1 - \theta$. If*

$$m = \frac{\|\mathbf{A} - \mathbf{A}_k\|_F^2}{(1 - \sqrt{1 - \theta})\gamma} + k, \text{ or } \gamma = \frac{\|\mathbf{A} - \mathbf{A}_k\|_F^2}{(1 - \sqrt{1 - \theta})(m - k)},$$

then

$$\|\text{bias}(\hat{\mathbf{x}})\|_2^2 \in \left[(1 - \theta) \|\text{bias}(\mathbf{x}^*)\|_2^2, \frac{1}{1 - \theta} \|\text{bias}(\mathbf{x}^*)\|_2^2 \right]$$

Proof. Denote $\alpha = 1/m-k$, $c^2 = 1 - \theta$ and $\Delta_k = \|\mathbf{A} - \mathbf{A}_k\|_F^2$. The assumptions of the theorem equivalently state that $(1 - c)\gamma = \alpha\Delta_k$. We apply Lemma 14 with $\mathbf{u} = \mathbf{H}_\gamma^{-1}\mathbf{x}_0$ and square all terms so that

$$\gamma'^2 \|\mathbf{u}\|_2^2 \leq \|\mathbf{M}\mathbf{u}\|_2^2 \leq \frac{\gamma^4}{\gamma'^2} \|\mathbf{u}\|_2^2.$$

Since $\gamma' = \gamma - \alpha\Delta_k$ we have $\gamma' = c\gamma$. Thus;

$$c^2\gamma^2 \|\mathbf{u}\|_2^2 \leq \|\mathbf{M}\mathbf{u}\|_2^2 \leq \frac{\gamma^2}{c^2} \|\mathbf{u}\|_2^2.$$

Finally, recall that $c^2 = 1 - \theta$ which obtains the stated bound. \square

Variance. The variance term is simpler to analyse thanks to the Löwner ordering. First we illustrate the sketched variance term:

Lemma 15. *The variance of the weights found from the sketched problem is: $\text{var}(\hat{\mathbf{x}}) = \sigma^2 \hat{\mathbf{H}}^{-1} \mathbf{A}^\top \mathbf{A} \hat{\mathbf{H}}^{-1}$.*

Proof. We will use from Equation (19) that $\mathbb{E}(\mathbf{y}) = \mathbf{A}\mathbf{x}_0$.

$$\text{var}(\hat{\mathbf{x}}) = (\hat{\mathbf{x}} - \mathbb{E}(\hat{\mathbf{x}})) (\hat{\mathbf{x}} - \mathbb{E}(\hat{\mathbf{x}}))^\top \quad (33)$$

$$= \left(\hat{\mathbf{H}}^{-1} \mathbf{A}^\top \mathbf{y} - \hat{\mathbf{H}}^{-1} \mathbf{A}^\top \mathbb{E}(\mathbf{y}) \right) \left(\hat{\mathbf{H}}^{-1} \mathbf{A}^\top \mathbf{y} - \hat{\mathbf{H}}^{-1} \mathbf{A}^\top \mathbb{E}(\mathbf{y}) \right)^\top \quad (34)$$

$$= \hat{\mathbf{H}}^{-1} \mathbf{A}^\top (\mathbf{y} - \mathbb{E}(\mathbf{y})) (\mathbf{y} - \mathbb{E}(\mathbf{y}))^\top \mathbf{A} \hat{\mathbf{H}}^{-1} \quad (35)$$

$$= \hat{\mathbf{H}}^{-1} \mathbf{A}^\top \text{var}(\mathbf{y}) \mathbf{A} \hat{\mathbf{H}}^{-1}. \quad (36)$$

Finally, we recognise that $\text{var}(\mathbf{y}) = \sigma^2 \mathbf{I}_n$ which establishes the claim. \square

Theorem 9. *Under the same assumptions as Theorem 8,*

$$\text{trace}(\text{var}(\mathbf{x}^*)) \leq \text{trace}(\text{var}(\hat{\mathbf{x}})) \leq \frac{1}{1 - \theta} \text{trace}(\text{var}(\mathbf{x}^*))$$

Proof. Lemma 5 and Equation (18)

$$\mathbf{H}_\gamma^{-1} \preceq \hat{\mathbf{H}}^{-1} \preceq \mathbf{H}_{\gamma'}^{-1} \leq \frac{\gamma}{\gamma'} \mathbf{H}_\gamma^{-1}.$$

The Löwner ordering above ensures that the following is also true:

$$\mathbf{H}_\gamma^{-1} \mathbf{A}^\top \mathbf{A} \mathbf{H}_\gamma^{-1} \preceq \hat{\mathbf{H}}^{-1} \mathbf{A}^\top \mathbf{A} \hat{\mathbf{H}}^{-1} \preceq \mathbf{H}_{\gamma'}^{-1} \mathbf{A}^\top \mathbf{A} \mathbf{H}_{\gamma'}^{-1}. \quad (37)$$

Multiplying through by the scalar σ^2 demonstrates that

$$\text{var}(\mathbf{x}^*) \leq \text{var}(\hat{\mathbf{x}}) \leq \text{var}(\mathbf{x}_{\gamma'}) \leq \frac{\gamma^2}{\gamma'^2} \text{var}(\mathbf{x}^*)$$

Finally, setting $\gamma' = c\gamma$ as in Theorem 8 obtains:

$$\text{var}(\mathbf{x}^*) \leq \text{var}(\hat{\mathbf{x}}) \leq \frac{1}{c^2} \text{var}(\mathbf{x}^*) = \frac{1}{1 - \theta} \text{var}(\mathbf{x}^*).$$

Since the trace maintains the Löwner ordering, we have established the claim. \square

MSE. We are finally in a position to bound the mean-squared error from using the FD ridge estimates rather than the exact weights. The upper bound is immediate since both upper bounds for bias and variance terms are $1/(1-\theta)$ multiples of the corresponding term over the exact weights. In Theorem 9 we have shown a slightly stronger bound for $\text{trace}(\text{var}(\mathbf{x}^*))$ than is necessary here, however, since $1 - \theta < 1$, Theorem 9 implies a lower bound of a $(1 - \theta)\text{trace}(\text{var}(\mathbf{x}^*))$ bound. Hence we obtain

$$(1 - \theta)\text{MSE}(\mathbf{x}^*) \leq \text{MSE}(\hat{\mathbf{x}}) \leq \frac{1}{1 - \theta} \text{MSE}(\mathbf{x}^*) \quad (38)$$

This is enough to prove the following theorem:

Theorem 10. *Under the same assumptions as Theorem 8,*

$$(1 - \theta)\text{MSE}(\mathbf{x}^*) \leq \text{MSE}(\hat{\mathbf{x}}) \leq \frac{1}{1 - \theta} \text{MSE}(\mathbf{x}^*)$$

B.3 Improved Bounds with Robust Frequent Directions

The structure of our proof maps allows us to apply it directly to the case when the Robust Frequent Directions algorithm is employed rather than vanilla FD. In this case, we have the following analogue of Theorem 7

Theorem 11 (Luo et al. (2019)). *Let $\mathbf{A} \in \mathbb{R}^{n \times d}$. The Robust Frequent Directions algorithm processes \mathbf{A} one row at a time and returns a matrix $\mathbf{B} \in \mathbb{R}^{m \times d}$ and a scalar $\delta \in \mathbb{R}$ such that*

$$\|\mathbf{A}^\top \mathbf{A} - (\mathbf{B}^\top \mathbf{B} + \delta \mathbf{I}_d)\|_2 \leq \frac{\|\mathbf{A} - \mathbf{A}_k\|_F^2}{2(m-k)},$$

or equivalently

$$\mathbf{A}^\top \mathbf{A} - \frac{\|\mathbf{A} - \mathbf{A}_k\|_F^2}{2(m-k)} \mathbf{I}_d \preceq \mathbf{B}^\top \mathbf{B} + \delta \mathbf{I}_d \preceq \mathbf{A}^\top \mathbf{A}.$$

With this guarantee in place we can easily prove the following theorem:

Theorem 12. *Let $\mathbf{B} = \text{RFD}(\mathbf{A}) \in \mathbb{R}^{m \times d}$. Let $\theta' \in (0, 1)$ be a parameter and set $c'^2 = 1 - \theta'$. If*

$$m = \frac{\|\mathbf{A} - \mathbf{A}_k\|_F^2}{2(1 - \sqrt{1 - \theta'})\gamma} + k, \text{ or } \gamma = \frac{\|\mathbf{A} - \mathbf{A}_k\|_F^2}{2(1 - \sqrt{1 - \theta'})(m - k)},$$

then

$$\begin{aligned} \|\text{bias}(\hat{\mathbf{x}})\|_2^2 &\in \left[(1 - \theta') \|\text{bias}(\mathbf{x}^*)\|_2^2, \frac{1}{1 - \theta'} \|\text{bias}(\mathbf{x}^*)\|_2^2 \right] \\ \text{trace}(\text{var}(\hat{\mathbf{x}})) &\in \left[\text{trace}(\text{var}(\mathbf{x}^*)) \frac{1}{1 - \theta'}, \text{trace}(\text{var}(\mathbf{x}^*)) \right] \\ \text{MSE}(\hat{\mathbf{x}}) &\in \left[(1 - \theta') \text{MSE}(\mathbf{x}^*), \frac{1}{1 - \theta'} \text{MSE}(\mathbf{x}^*) \right] \end{aligned}$$

Proof. Let $\hat{\mathbf{H}}_{\delta, \gamma} = \mathbf{B}^\top \mathbf{B} + (\delta + \gamma) \mathbf{I}_d$. Let $\hat{\mathbf{x}} = \hat{\mathbf{H}}^{-1} \mathbf{A}^\top \mathbf{b}$ be the estimated weights. Again let $\Delta_k = \|\mathbf{A} - \mathbf{A}_k\|_F^2$ and $\alpha = 1/(m-k)$. We take $\gamma' = \gamma - \alpha \Delta_k/2$.

Bias Term. The same approach as Lemma 12 establishes that $\text{bias}(\hat{\mathbf{x}}) = (\hat{\mathbf{H}}_{\delta, \gamma}^{-1} \mathbf{A}^\top \mathbf{A} - \mathbf{I}_d) \mathbf{x}_0$. Again we use the same trick of multiplying by the identity to obtain $\text{bias}(\hat{\mathbf{x}}) = (\hat{\mathbf{H}}_{\delta, \gamma}^{-1} \mathbf{A}^\top \mathbf{A} - \mathbf{I}_d) \mathbf{H}_\gamma \mathbf{H}_\gamma^{-1} \mathbf{x}_0$. Thus it suffices to bound the extremal eigenvalues of $\mathbf{M} = (\hat{\mathbf{H}}_{\delta, \gamma}^{-1} \mathbf{A}^\top \mathbf{A} - \mathbf{I}_d) \mathbf{H}_\gamma$. We can invoke exactly the same proof as in Lemma 14 but note that the bounds:

$$\lambda_{\max}(\mathbf{M}) \leq \frac{\gamma}{\gamma'} \tag{39}$$

$$\lambda_{\min}(\mathbf{M}) \geq \gamma'. \tag{40}$$

$$\tag{41}$$

Let $\mathbf{u} = \mathbf{H}_\gamma^{-1} \mathbf{x}_0$ and $1 - c' = \alpha \Delta_k/2$. Hence, $\gamma' = c' \gamma$. Following the proof of Theorem 8 we establish that:

$$c'^2 \gamma^2 \|\mathbf{u}\|_2^2 \leq \|\mathbf{M} \mathbf{u}\|_2^2 \leq \frac{\gamma^2}{c'^2} \|\mathbf{u}\|_2^2.$$

Recall that $c'^2 = 1 - \theta'$ so that we obtain the stated result.

Variance and MSE. Again repeat the argument of Theorem 9 but recall that our altered values of γ/γ' mean that the upper bound is $1/(1-\theta')$. The MSE result is then immediate, as before by combining the bias and variance terms. \square

Remark 3. *To understand the relation between the bias-variance tradeoff using FD compared to RFD we need to account for how $1 - \theta$ and $1 - \theta'$ interact. This is observed through some fairly simple algebra: from the definition of c we can show that $c = \gamma'/\gamma$. Similarly,*

$$c' = 1 - \frac{\alpha \Delta_k}{2\gamma}$$

which, by recalling that $\alpha\Delta_k = (1-c)\gamma$ we observe that $c' = \frac{1+c}{2}$. By squaring, we have

$$\begin{aligned} 1 - \theta' &= \left(\frac{1+c}{2}\right)^2 \\ &= \frac{2 - \theta + 2\sqrt{1-\theta}}{4} \\ &\geq 1 - \theta \text{ for } \theta \in [0, 1]. \end{aligned}$$

Therefore, the $1 - \theta'$ relative error bounds are tighter than the $1 - \theta$ bounds.

C Iterative Frequent Directions Ridge Regression: Theory

We present the details for the results outlined in Section 4. Before presenting the theory, we set up some notation and some preliminary proofs to aid the presentation. Recall Equation (1)

$$f(\mathbf{x}) = \frac{1}{2}\|\mathbf{A}\mathbf{x} - \mathbf{b}\|_2^2 + \frac{\gamma}{2}\|\mathbf{x}\|_2^2$$

and the task is to find, or estimate $\arg \min_{\mathbf{x}} f(\mathbf{x})$. The optimal solution to the above problem is

$$\mathbf{x}^* = (\mathbf{A}^\top \mathbf{A} + \gamma \mathbf{I}_d)^{-1} \mathbf{A}^\top \mathbf{b}. \quad (42)$$

The gradient of $f(\mathbf{x})$ is

$$\nabla f(\mathbf{x}) = (\mathbf{A}^\top \mathbf{A} + \gamma \mathbf{I}_d) \mathbf{x} - \mathbf{A}^\top \mathbf{b}. \quad (43)$$

Note that $\nabla f(\mathbf{x}) \in \mathbb{R}^d$ and can be applied in $O(nd)$ time. That is, $\mathbf{A}^\top \mathbf{A} + \gamma \mathbf{I}_d$ need not be explicitly computed as the matrix-vector products can be evaluated from right to left to avoid the matrix-matrix multiplication. Recall that $\mathbf{H}_\gamma = \mathbf{A}^\top \mathbf{A} + \gamma \mathbf{I}_d$ is the Hessian matrix of second-derivatives of $f(\mathbf{x})$. Computing \mathbf{H}_γ requires $O(nd^2)$ time and $O(d^2)$ space.

Rather than computing \mathbf{H}_γ , we estimate it through the FD sketch. Recall that $\hat{\mathbf{H}} = \mathbf{B}^\top \mathbf{B} + \gamma \mathbf{I}_d$ is our approximation to \mathbf{H}_γ . Although Algorithm 1 uses \mathbf{H}^{-1} , this need not be computed explicitly and we only need its behaviour as an operator. This can be understood through the Woodbury inverse lemma which we defer for now and present in Section D. The proof of Theorem ? roughly follows a standard gradient descent-type proof so we need a few preliminary results.

Lemma 16. $\nabla f(\mathbf{x}) = \mathbf{H}(\mathbf{x} - \mathbf{x}^*)$

Proof.

$$\begin{aligned} \nabla f(\mathbf{x}) &= \mathbf{A}^\top (\mathbf{A}\mathbf{x} + \mathbf{b}) + \gamma \mathbf{x} \\ &= (\mathbf{A}^\top \mathbf{A} + \gamma \mathbf{I}_d) \mathbf{x} + \mathbf{A}^\top \mathbf{b} \\ &= (\mathbf{A}^\top \mathbf{A} + \gamma \mathbf{I}_d) (\mathbf{x} - \mathbf{x}^*) \\ &= \mathbf{H} (\mathbf{x} - \mathbf{x}^*) \end{aligned}$$

where the penultimate equation follows from the normal equations: $(\mathbf{A}^\top \mathbf{A} + \gamma \mathbf{I}_d) \mathbf{x}^* = \mathbf{A}^\top \mathbf{b}$. \square

The following lemma represents the current iterate $\mathbf{x}^{(t+1)}$ as a function of the previous iterate's distance from the optimal solution.

Lemma 17. *The sequence of iterates $\{\mathbf{x}^{(t+1)}\}_{i \geq 0}$ follows:*

$$\mathbf{x}^{(t+1)} - \mathbf{x}^* = \left(\mathbf{I}_d - \hat{\mathbf{H}}^{-1} \mathbf{H}\right) \left(\mathbf{x}^{(t)} - \mathbf{x}^*\right). \quad (44)$$

Proof. Applying Lemma 16 to the iterates as defined in (7) we obtain:

$$\mathbf{x}^{(t+1)} - \mathbf{x}^* = \mathbf{x}^{(t)} - \mathbf{x}^* - \hat{\mathbf{H}}^{-1} \mathbf{H} \left(\mathbf{x}^{(t)} - \mathbf{x}^*\right)$$

which yields the claim after factorisation. \square

Taking the norm of both sides of Equation 44 and invoking submultiplicativity we have

$$\left\| \mathbf{x}^{(t+1)} - \mathbf{x}^* \right\|_2 \leq \left\| \mathbf{I}_d - \hat{\mathbf{H}}^{-1} \mathbf{H} \right\|_2 \left\| \mathbf{x}^{(t)} - \mathbf{x}^* \right\|_2.$$

On the right hand side, the first 2-norm is the spectral norm over matrices, while the second 2-norm is the Euclidean norm over vectors. Hence, to show $\left\| \mathbf{x}^{(t+1)} - \mathbf{x}^* \right\|_2 \leq \left\| \mathbf{x}^{(t)} - \mathbf{x}^* \right\|_2$ it suffices to show $\left\| \mathbf{I}_d - \hat{\mathbf{H}}^{-1} \mathbf{H} \right\|_2 < 1$.

Lemma 18. *If $2\alpha\Delta_k < \gamma$, then $\left\| \mathbf{I}_d - \hat{\mathbf{H}}^{-1} \mathbf{H} \right\|_2 < 1$*

Proof. Since $\hat{\mathbf{H}}^{-1} \mathbf{H}$ is similar to $\mathbf{E} = \hat{\mathbf{H}}^{-1/2} \mathbf{H} \hat{\mathbf{H}}^{-1/2}$, it has the same eigenvalues. Hence we can bound $\left\| \mathbf{I}_d - \mathbf{E} \right\|_2$ instead. By definition, spectral norm asks for:

$$\left\| \mathbf{I}_d - \mathbf{E} \right\|_2 = \max_{\mathbf{u}: \|\mathbf{u}\|=1} |\mathbf{u}^\top (\mathbf{I}_d - \mathbf{E}) \mathbf{u}|$$

so we need to show that $\max_{\mathbf{u}} |1 - \mathbf{u}^\top \mathbf{E} \mathbf{u}| < 1$. To do so, we need a few properties of the FD sketch. Let $\alpha = 1/m-k$ and $\Delta_k = \|\mathbf{A} - \mathbf{A}_k\|_F^2$ so that Theorem 7 with the added regularisation ensures (see Equation (9)):

$$\mathbf{A}^\top \mathbf{A} + (\gamma - \alpha\Delta_k) \mathbf{I}_d \preceq \mathbf{B}^\top \mathbf{B} + \gamma \mathbf{I}_d \preceq \mathbf{A}^\top \mathbf{A} + \gamma \mathbf{I}_d. \quad (45)$$

Provided that $\gamma > \alpha\Delta_k \mathbf{I}_d$, all of the above terms are lower bounded by $\mathbf{0}_{d \times d}$. This is equivalent to saying that all eigenvalues are positive, hence the matrices are full rank and inverses are well-defined.

Denote $\gamma' = \gamma - \alpha\Delta_k$. Lemma 8 shows that

$$\frac{\gamma'}{\gamma} (\mathbf{A}^\top \mathbf{A} + \gamma \mathbf{I}_d) \preceq \mathbf{A}^\top \mathbf{A} + \gamma' \mathbf{I}_d. \quad (46)$$

Let $q = \alpha\Delta_k/\gamma > 0$ so that $\frac{\gamma'}{\gamma} = 1 - q$. Invoking (45) we obtain the ordering:

$$(1 - q) (\mathbf{A}^\top \mathbf{A} + \gamma \mathbf{I}_d) \preceq \mathbf{B}^\top \mathbf{B} + \gamma \mathbf{I}_d \preceq \mathbf{A}^\top \mathbf{A} + \gamma \mathbf{I}_d. \quad (47)$$

Now use Point 2 Section D.1 on all three terms in (47) with $\mathbf{C} = \hat{\mathbf{H}}^{-1/2}$. Again, since all of the matrices in question are symmetric positive definite, they have unique symmetric positive definite square roots so we are free to apply the Löwner multiplication order.

$$(1 - q) \hat{\mathbf{H}}^{-1/2} (\mathbf{A}^\top \mathbf{A} + \gamma \mathbf{I}_d) \hat{\mathbf{H}}^{-1/2} \preceq \mathbf{I}_d \preceq \hat{\mathbf{H}}^{-1/2} (\mathbf{A}^\top \mathbf{A} + \gamma \mathbf{I}_d) \hat{\mathbf{H}}^{-1/2}. \quad (48)$$

The above equation also implies that $\hat{\mathbf{H}}^{-1/2} (\mathbf{A}^\top \mathbf{A} + \gamma \mathbf{I}_d) \hat{\mathbf{H}}^{-1/2} \preceq \frac{1}{1-q} \mathbf{I}_d$. Hence, we also have

$$\mathbf{I}_d \preceq \hat{\mathbf{H}}^{-1/2} (\mathbf{A}^\top \mathbf{A} + \gamma \mathbf{I}_d) \hat{\mathbf{H}}^{-1/2} \preceq \frac{1}{1-q} \mathbf{I}_d. \quad (49)$$

The Löwner ordering also ensures that $\lambda_{\min}(\mathbf{M}) \mathbf{I} \preceq \mathbf{M} \preceq \lambda_{\max}(\mathbf{M}) \mathbf{I}$. Hence, we have shown that

$$\lambda_i(\hat{\mathbf{H}}^{-1/2} (\mathbf{A}^\top \mathbf{A} + \gamma \mathbf{I}_d) \hat{\mathbf{H}}^{-1/2}) \in \left[1, \frac{1}{1-q} \right]. \quad (50)$$

Finally, it remains to ensure that $\max_{\mathbf{u}} |1 - \mathbf{u}^\top \mathbf{E} \mathbf{u}| < 1$. Since all $\lambda_i(\mathbf{E}) \geq 1$, the largest displacement occurs at $\lambda_{\max}(\mathbf{E})$. Therefore, q must be set so that

$$\left| 1 - \frac{1}{1-q} \right| < 1$$

that is,

$$\frac{q}{1-q} < 1 \quad (51)$$

which occurs provided $q \in (0, 1/2)$ and is thus satisfied by the assumption $2\alpha\Delta_k < \gamma$. \square

The preceding result can be used iteratively. In summary, the following theorem establishes that choosing $\gamma > 2\alpha\Delta_k$ ensures the distance from $\mathbf{x}^{(t+1)}$ to \mathbf{x}^* is at most an $\alpha\Delta_k/\gamma$ factor smaller than that of $\mathbf{x}^{(t)}$ to \mathbf{x}^* .

Theorem 13. *Let $b \in (0, 1/2)$ and suppose that $\alpha\Delta_k = b\gamma$. The iterative sketch algorithm for regression with Frequent Directions satisfies*

$$\|\mathbf{x}^{(t+1)} - \mathbf{x}^*\|_2 \leq \left(\frac{b}{1-b}\right)^{t+1} \|\mathbf{x}^*\|_2 \quad (52)$$

Proof. Let $\beta = \frac{q}{1-q}$ as in Equation (51). Hence, $\beta = \alpha\Delta_k/\gamma'$. Assuming that $\alpha\Delta_k = b\gamma$ so $\gamma' = (1-b)\gamma$ means $\beta = 1-c/c$. Since $b < 1/2$ we have $\alpha\Delta_k < \gamma/2$ hence Lemma 18 establishes that $\|\mathbf{I}_d - \hat{\mathbf{H}}^{-1}\mathbf{H}\|_2 \leq \beta$. Thus, $\|\mathbf{x}^{(t+1)} - \mathbf{x}^*\|_2 \leq \beta \|\mathbf{x}^{(t)} - \mathbf{x}^*\|_2$. By induction, we can iterate this argument to obtain $\|\mathbf{x}^{(t+1)} - \mathbf{x}^*\|_2 \leq \beta^{t+1} \|\mathbf{x}^*\|_2$ which follows by recalling that $\mathbf{x}^{(0)} = \mathbf{0}_d$. \square

C.1 Iterative Ridge Regression with Robust Frequent Directions

We can slot the robust variant of FD into the iterative framework. The proofs follow on as before with a mild adjusting of the constants. Again, the key technical detail is, for $\hat{\mathbf{H}}_{\delta,\gamma} = \mathbf{B}^\top\mathbf{B} + (\delta + \gamma)\mathbf{I}_d$, establishing that $\|\mathbf{I}_d - \hat{\mathbf{H}}_{\delta,\gamma}\mathbf{H}\|_2 < 1$. The improvement over using RFD is that we can weaken the hypothesis necessary for the result.

Lemma 19. *If $\alpha\Delta_k < \gamma$, then $\|\mathbf{I}_d - \hat{\mathbf{H}}_{\delta,\gamma}^{-1}\mathbf{H}\|_2 < 1$*

Proof. We follow the proof of Lemma 18 almost exactly but with the following modifications. Equation (45) we use the RFD guarantee which tightens the bounds to

$$\mathbf{A}^\top\mathbf{A} + \left(\gamma - \frac{\alpha\Delta_k}{2}\right)\mathbf{I}_d \preceq \mathbf{B}^\top\mathbf{B} + \gamma\mathbf{I}_d \preceq \mathbf{A}^\top\mathbf{A} + \gamma\mathbf{I}_d.$$

Then take $\gamma' = \gamma - \alpha\Delta_k/2$ and $q = \alpha\Delta_k/2\gamma$. Hence, $\gamma'/\gamma = 1 - q$ as before. As in Equation (51), we require $q/(1-q) < 1$ so $q < 1/2$. By assumption $\alpha\Delta_k < \gamma$ so $q < 1/2$ is satisfied. \square

Theorem 14. *Let $b \in (0, 1)$ and suppose that $\alpha\Delta_k = b\gamma$. The iterative sketch algorithm for regression with Robust Frequent Directions satisfies*

$$\|\mathbf{x}^{(t+1)} - \mathbf{x}^*\|_2 \leq \left(\frac{b}{2-b}\right)^{t+1} \|\mathbf{x}^*\|_2 \quad (53)$$

Proof. Same proof as Theorem 13 except noting that

$$\begin{aligned} \beta &= \frac{q}{1-q} \\ &= \frac{\alpha\Delta_k/2\gamma}{(2\gamma - \alpha\Delta_k)/2\gamma} \\ &= \frac{\alpha\Delta_k}{2\gamma - \alpha\Delta_k} \\ &= \frac{b}{2-b} \end{aligned}$$

\square

C.2 Further Experimental Results

In Figures 4 and 5 we plot the results for the experiments as described in Section 4. The conclusions remain the same as in Section 4 with Robust Frequent Directions providing the best small-space preconditioner, followed by Frequent Directions and the iterative Hessian Sketch with SJLT (IHS:SJLT). Although IHS:SJLT appears competitive, it requires a new sketch for every gradient step. While these can be computed in parallel on viewing the data, it is still many more sketches than the single sketch required by the (Robust) Frequent Directions methods. When one is restricted to a single sketch, the SJLT does not perform at a similar level to the (Robust) Frequent Directions methods.

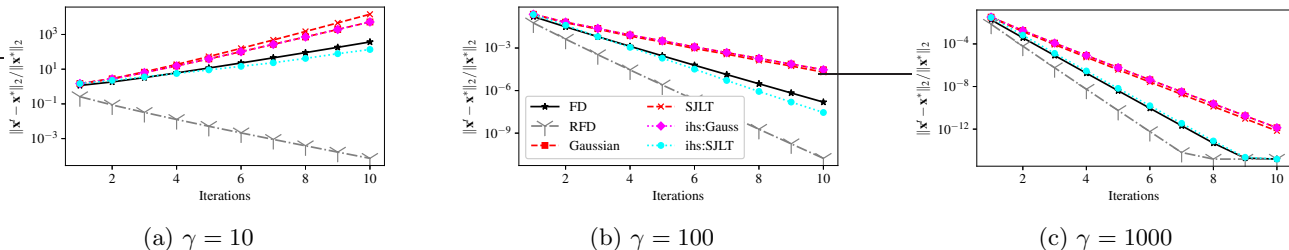


Figure 4: Performance of the iterative ridge regression algorithm (Algorithm 1) on the ForestCover dataset.

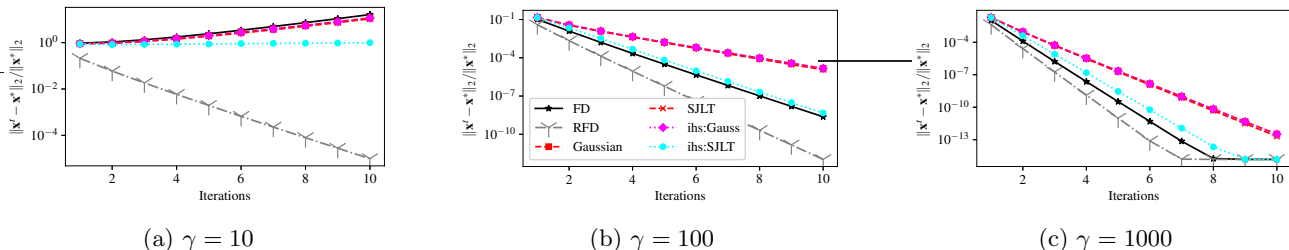


Figure 5: Performance of the iterative ridge regression algorithm (Algorithm 1) on the YearPredictions dataset.

D Spectral Results and Löwner Ordering

D.1 Löwner Ordering Properties

A matrix $\mathbf{A} \in \mathbb{R}^{d \times d}$ is symmetric positive definite (p.d.) if and only if it is symmetric and positive definite. Positive definite means that $\mathbf{A} \succ \mathbf{0}$, equivalently, $\mathbf{x}^\top \mathbf{A} \mathbf{x} > 0$. Applied to covariance matrices of full rank, for example $\mathbf{A}^\top \mathbf{A}$ this is equivalent to asking for $\|\mathbf{A} \mathbf{x}\|_2^2 > 0$. The strictness of each of the above inequalities can be relaxed to allow equality if we permit symmetric positive *semi* definite matrices (spsd) For any two spsd matrices we write $\mathbf{B} \preceq \mathbf{A}$ if and only if $\mathbf{A} - \mathbf{B} \succeq \mathbf{0}_{d \times d}$.

Some facts which can be found at (<https://www.cs.ubc.ca/~nickhar/W12/NotesMatrices.pdf>) or in *Appendix A: Aspects of Semidefinite Programming (De Klerk, 2006)* are :

Fact 1. Let $\mathbf{A}, \mathbf{B}, \mathbf{C}$ be arbitrary symmetric positive definite matrices.

1. If $\mathbf{A} \preceq \mathbf{B}$ then it is not strictly true that $\mathbf{A}^2 \preceq \mathbf{B}^2$. This is the case if the matrices commute, however.
2. If $\mathbf{A} \preceq \mathbf{B}$ then $\mathbf{C} \mathbf{A} \mathbf{C}^\top \preceq \mathbf{C} \mathbf{B} \mathbf{C}^\top$. In fact, this is an if and only if when \mathbf{C} is of full rank.
3. Let λ_{\min} and λ_{\max} be the smallest and largest eigenvalues of \mathbf{A} . Then $\lambda_{\min} \mathbf{I}_d \preceq \mathbf{A} \preceq \lambda_{\max} \mathbf{A}$.
4. If $\mathbf{A} \preceq \mathbf{B}$ then $\text{trace}(\mathbf{A}) \leq \text{trace}(\mathbf{B})$
5. If $\mathbf{A} \preceq \mathbf{B}$ then $\mathbf{B}^{-1} \preceq \mathbf{A}^{-1}$

D.2 Matrix Results

We need two further standard results:

Lemma 20. A positive definite matrix has a unique positive definite square root which is symmetric.

This lemma allows us to take positive definite matrix $\mathbf{Q} = \mathbf{C} \mathbf{C}^\top$ (or its) inverse and invoke property 2 for the Löwner ordering. This is because the square root is additionally symmetric so $\mathbf{C} = \mathbf{C}^\top$. We repeatedly apply this result on matrices such as $\mathbf{H}_\gamma, \mathbf{H}_\gamma^{-1}$. For square matrices \mathbf{X}, \mathbf{Y} , the generalized Rayleigh quotient is $R(\mathbf{X}, \mathbf{Y}, \mathbf{u}) = \mathbf{u}^\top \mathbf{X} \mathbf{u} / \mathbf{u}^\top \mathbf{Y} \mathbf{u}$.

Lemma 21. The largest (smallest) eigenvalue of a psd matrix \mathbf{X} maximises (minimises) the Rayleigh Quotient over \mathbf{X} :

$$\lambda_{\max} := \max_{\mathbf{u}: \|\mathbf{u}\|_2=1} R(\mathbf{X}, \mathbf{Y}, \mathbf{u})$$

$$\lambda_{\min} := \min_{\mathbf{u}: \|\mathbf{u}\|_2=1} R(\mathbf{X}, \mathbf{Y}, \mathbf{u})$$

E Miscellaneous

- Synthetic Data.** We adapt the synthetic dataset found in Section 4 (Shi & Phillips, 2020). First we set the *effective dimension* $R = \lfloor 0.1 \cdot d + 0.5 \rfloor$. This is then used to set the number of nonzero indices in the ground truth vector \mathbf{x}_0 and the number of standard deviations for the multivariate normal distribution used in generating \mathbf{A} . The first R components of \mathbf{x}_0 are sampled from a standard normal distribution, \mathbf{x}_0 is then normalised to unit length. The samples (rows) \mathbf{A}_i are generated by a normal distribution with standard deviation $\exp(-(i-1)^2/R^2)$ for $i = 1 : n$. Finally, we rotate \mathbf{A} by a discrete cosine transform. We sample noise a noise vector $\boldsymbol{\varepsilon}$ with $\varepsilon_i \sim \mathcal{N}(0, 2^2)$ and set $\mathbf{y} = \mathbf{A}\mathbf{x}_0 + \boldsymbol{\varepsilon}$.
- Gaussian Random Projection.** The sketch $\mathbf{SA} \in \mathbb{R}^{m \times d}$ is generated by choosing $\mathbf{R}_{ij} \sim \mathcal{N}(0, 1)$ and then taking $\mathbf{S} = \mathbf{R}/\sqrt{m}$. If $m = O(d\rho^{-2} \log(1/\delta))$, then \mathbf{S} is a $(1 \pm \rho)$ - ℓ_2 subspace embedding for \mathbf{A} (Woodruff, 2014).
- SJLT.** We use the SJLT as it compromises a small sketch dimension m against the speed at which one can apply the transform. The SJLT is a concatenation of s CountSketch matrices which are defined as follows Clarkson & Woodruff (2017). Let $\mathbf{S} = \mathbf{0}_{m \times n}$. For every column $c \in [n]$, choose a row r uniformly at random from $[m]$. Randomly set $\mathbf{S}_{rc} = \pm 1$ each with probability $1/2$. It has been shown that such an \mathbf{S} provides a $(1 \pm \rho)$ -subspace embedding with probability at least $1 - \delta$ if $m = O(d^2 \rho^{-2} \delta^{-1})$. This is not favourable if d is moderate-to-large and is only suitable for constant probability of success due to the $1/\delta$ dependency. However, the CountSketch can be applied to input \mathbf{A} easily as it is observed. In order to retain the benefits of CountSketch but to improve on its weaker space dependency, Nelson & Nguyễn (2013) showed that by stacking $s > O(1/\rho)$ CountSketch matrices of size m/s and choosing $m = O(d\rho^{-2} \text{polylog}(d/\delta))$ then a $(1 \pm \rho)$ - subspace embedding can be achieved. The time to apply the embedding is then s times the time required to apply a CountSketch, so is still close to the time taken to read the data. We refer to this construction as an SJLT which is a factor of d better in the projection dimension m and exponentially better for the failure probability than CountSketch. Our experiments take $s = 10$.